



Khudhur, F.W.K. , MacDonald, J.M., Macente, A. and Daly, L. (2022) The utilization of alkaline wastes in passive carbon capture and sequestration: promises, challenges and environmental aspects. *Science of the Total Environment*, 823, 153553. (doi: [10.1016/j.scitotenv.2022.153553](https://doi.org/10.1016/j.scitotenv.2022.153553)).

This is the Author Accepted Manuscript.

There may be differences between this version and the published version. You are advised to consult the publisher's version if you wish to cite from it.

<http://eprints.gla.ac.uk/263798/>

Deposited on: 28 January 2022

Enlighten – Research publications by members of the University of Glasgow  
<http://eprints.gla.ac.uk>

# 1 The Utilization of Alkaline Wastes in Passive Carbon Capture 2 and Sequestration: Promises, Challenges and Environmental 3 Aspects

4 Khudhur, Faisal W. K: University of Glasgow, School of Geographical and  
5 Earth Sciences

6 Macente, Alice: University of Glasgow, School of Geographical and Earth  
7 Sciences; University of Strathclyde, Department of Civil and  
8 Environmental Engineering

9 MacDonald, John: University of Glasgow, School of Geographical and  
10 Earth Sciences

11 Daly, Luke: University of Glasgow, School of Geographical and Earth  
12 Sciences; University of Sydney, Australian Centre for Microscopy and  
13 Microanalysis; University of Oxford, Department of Materials

14 Journal: accepted for publication in *Science of the Total*  
15 *Environment*

## 16 Abstract

17 Alkaline wastes have been the focus of many studies as they act as CO<sub>2</sub> sinks  
18 and have the potential to offset emissions from mining and steelmaking industries.  
19 Passive carbonation of alkaline wastes mimics natural silicate weathering and  
20 provides a promising alternative pathway for CO<sub>2</sub> capture and storage as carbonates,  
21 requiring marginal human intervention when compared to ex-situ carbonation. This  
22 review summarizes the extant research that has investigated the passive carbonation  
23 of alkaline wastes, namely ironmaking and steelmaking slag, mine tailings and  
24 demolition wastes, over the past two decades. Here we report different factors that

25 affect passive carbonation to address challenges that this process faces and to identify  
26 possible solutions. We identify avenues for future research such as investigating how  
27 passive carbonation affects the surrounding environment through interaction with the  
28 biosphere and the hydrosphere. Future research should also consider economic  
29 analyses to provide investors with an in-depth understanding of passive carbonation  
30 techniques. Based on the reviewed materials, we conclude that passive carbonation  
31 can be an important contributor to climate change mitigation strategies, and its  
32 potential can be intensified by applying simple waste management practices.

33 **Keywords:** Carbon sequestration; mineral carbonation; slag; tailings; artificial soil;  
34 silicate weathering.

35

## 36 1. Introduction

37 The United Nations Statistics Department (UNSD) defines wastes as  
38 substances that are not primary products (produced for the market) and are meant to  
39 be disposed of as the generators have no use for them in consumption, production,  
40 and transformation (UNSD, 2016). Several industries generate wastes of alkaline  
41 nature. For example, ironmaking and steelmaking produce slag, aluminium production  
42 produces red mud, mining operations produce tailings and buildings demolition  
43 produces demolition wastes (Renforth, 2019). The alkaline nature of these wastes is  
44 attributed to their content of alkaline earth oxides, notably calcium oxide (CaO) and  
45 magnesium oxide (MgO); both can hydrate to produce  $\text{Ca(OH)}_2$  and  $\text{Mg(OH)}_2$ ,  
46 respectively, which act as alkalinity sources (Riley and Mayes, 2015; Roadcap et al.,  
47 2006, 2005). High pH is associated with several leachates from alkaline residues  
48 (Mayes et al., 2006; Meyer, 1980). Such leachates cause several environmental  
49 problems like smothering of littoral aquatic habitats and reduction of light penetration  
50 to benthic producers (Mayes et al., 2008a). Leachates also contain metals at  
51 concentrations that are harmful to macrophytes and other organisms in the food web  
52 and can cause contamination of drinking water sources and agricultural land pollution  
53 (Gao et al., 2021; Olszewska et al., 2016). Alkaline wastes can contain high  
54 concentrations of ecotoxic metals such as lead and chromium (VI) which can reach  
55 978 mg/kg and 851 mg/kg, respectively (Hu et al., 2020). Such metals can be released  
56 into the environment as a result of infiltration by rain or other water sources (Gomes  
57 et al., 2016; Mayes et al., 2011).

58 Historically, alkaline wastes have been either abandoned near production sites  
59 or collected into storage facilities (Riley et al., 2020; Santini and Banning, 2016).  
60 Recently, due to the increased awareness of sustainability and the drive towards a

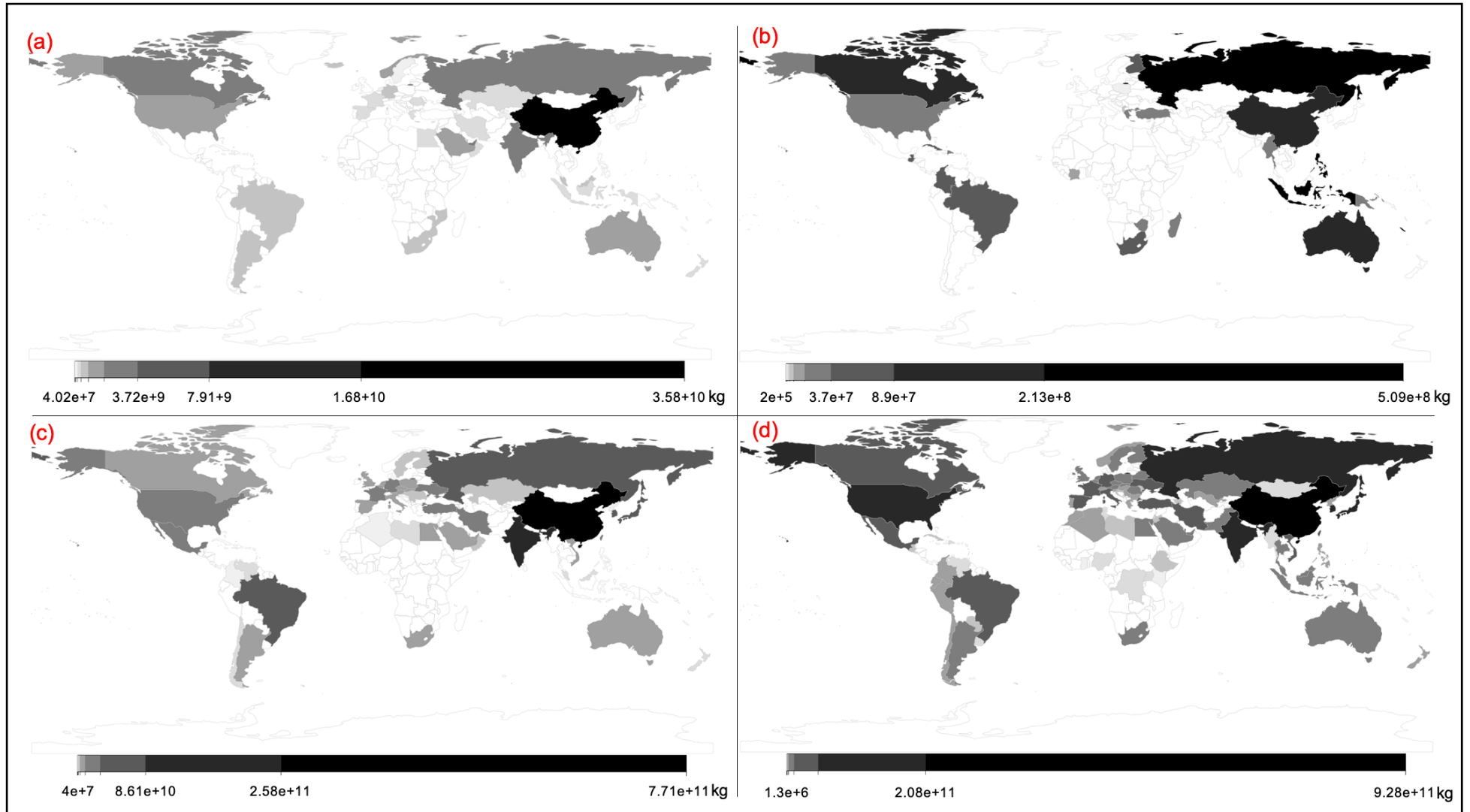
61 circular economy, there have been several attempts to utilize alkaline wastes,  
62 particularly in road construction, land restoration, element recovery and more recently  
63 in carbon capture and sequestration (CCS) (Gomes et al., 2016; Santini and Banning,  
64 2016; Sorlini et al., 2012). The latter idea gained considerable attention as it mimics  
65 natural weathering (Kelemen et al., 2020, 2011; National Academies of Sciences  
66 Engineering and Medicine, 2019). Natural silicate weathering and subsequent  
67 carbonate precipitation are critical processes that control the atmospheric CO<sub>2</sub>  
68 concentration (Daval, 2018; Huh, 2003; Schuiling and Krijgsman, 2006). This process  
69 captures carbon at a rate of 1-2.8 g C m<sup>-2</sup> y<sup>-1</sup> while mineral carbonation of alkaline  
70 wastes captures carbon at rates that are orders of magnitude greater than this value  
71 (Amiotte Suchet et al., 2003; Gaillardet et al., 1999; Huh, 2003; Oskierski et al., 2013;  
72 Wilson et al., 2014).

73         The high production of metals throughout the world (Fig. 1) results in vast  
74 amounts of alkaline wastes, which was estimated to be produced at an annual rate of  
75  $7 \times 10^{12}$  -  $1.7 \times 10^{13}$  kg y<sup>-1</sup> globally and projected to increase during this century  
76 (Renforth et al., 2011; Renforth, 2019). Power et al. (2013) estimated that ultramafic  
77 wastes can capture up to  $1.75 \times 10^{11}$  kg CO<sub>2</sub> y<sup>-1</sup>, while Renforth et al. (2011b)  
78 estimated a CO<sub>2</sub> uptake potential of  $7.0 \times 10^{11}$  kg CO<sub>2</sub> y<sup>-1</sup> when considering other  
79 alkalinity sources such as demolition wastes and slag. Renforth (2019) calculated that  
80 CO<sub>2</sub> emissions associated with different shared socioeconomic pathways and showed  
81 that by 2100, the CO<sub>2</sub> emissions are projected to be between  $2.4 \times 10^{13}$  kg CO<sub>2</sub> y<sup>-1</sup>  
82 and  $1.26 \times 10^{14}$  kg CO<sub>2</sub> y<sup>-1</sup>, and alkaline wastes carbonation can mitigate between 5%  
83 and 12% of these emissions. Carbonation of wastes has also been associated with  
84 reducing their environmental hazards since it reduces the pH of leachates as well as  
85 the concentration of metals in leachates, though the latter was found to depend on the

86 degree of carbonation (Gomes et al., 2016; Van Gerven et al., 2006). As CO<sub>2</sub>  
87 mineralisation can offset the emissions of mining and steelmaking industries, it can  
88 result in several economic, societal and biological benefits that are aligned with  
89 different sustainable development goals, including good health and well-being, climate  
90 action, sustainable cities and communities and quality of life on land (Olabi et al.,  
91 2022).

92         The Intergovernmental Panel on Climate Change (IPCC) explains that to avoid  
93 catastrophic consequences of global warming, the global temperature must not  
94 increase by more than 1.5 °C by the end of this century, compared to the preindustrial  
95 period (1850-1900) (IPCC, 2021). Here, we study the opportunities and challenges of  
96 using passive carbonation as a simple and inexpensive climate change mitigation  
97 pathway. This paper is structured as follows: Section 2 describes the carbonation  
98 reactions, including how different conditions can affect the CO<sub>2</sub> uptake; Section 3  
99 reviews relevant studies of passive carbonation in slag, demolition wastes and tailings.  
100 We focus on slag, construction and demolition wastes, nickel tailings, chrysotile tailing,  
101 diamond tailings and red mud. Large stocks of these materials are available  
102 worldwide, and except for chrysotile, these materials are produced in large amounts.  
103 These wastes have been passively managed for a period long enough to allow for  
104 passive carbonation to be observed. Additionally, they have favorable chemistry that  
105 enables them to offset emissions of mining and steelmaking industries (Bullock et al.,  
106 2022). Section 4 summarizes some limitations that reduce CO<sub>2</sub> uptake in alkaline  
107 wastes, and Section 5 suggests some large-scale methods that can utilize passive  
108 carbonation. Based on our engagement with the studied articles, we propose several  
109 areas of further research, particularly related to life cycle assessment, economic

- 110 analysis and the relation of passive carbonation to the surrounding environment.
- 111 These areas are discussed in Section 6.



112

113  
114

Fig. 1. Production (in kg) of (a) primary aluminum, (b) nickel, (c) pig iron, and (d) crude steel in 2018. White areas represent countries for which data were not available. Data from World Mineral Statistics contributed by permission of the British Geological Survey (Brown et al., 2020).



## 115 **2. Mineral carbonation chemistry**

### 116 **2.1 Carbonation reactions**

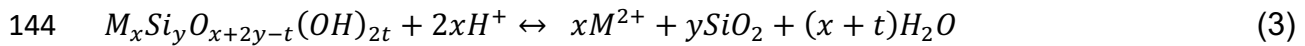
117 Alkaline wastes contain metal oxides, notably CaO and MgO, as well as other  
118 minerals such as brucite ( $Mg(OH)_2$ ), serpentine ( $Mg_3Si_2O_5(OH)_4$ ), forsterite ( $Mg_2SiO_4$ )  
119 and wollastonite ( $CaSiO_3$ ) (Power et al., 2013). These minerals can be carbonated  
120 through either dry or aqueous methods. Although the dry carbonation of these  
121 minerals is spontaneous (e.g., for carbonation of serpentine and wollastonite, Liu et  
122 al. (2021) reported  $\Delta G$  values of -16.9 kJ/mol, and - 44.6kJ/mol, respectively), it has a  
123 low rate, which can only be improved through different pre-processing steps. These  
124 pre-processing steps aim to release the MgO and CaO through energy-intensive  
125 processes before  $CO_2$  uptake can take place (Zevenhoven and Kavaliauskaite, 2004).  
126 Consequently, dry carbonation is unlikely to be commercialised (Huijgen and Comans,  
127 2005). Alternatively, aqueous carbonation has been reported to occur passively at  
128 different sites worldwide (Power et al., 2014). The first step in this method involves  
129  $CO_2$  dissolution and speciation according to the pH of the solution in which carbonation  
130 occurs. Archer (2007) explained that when water is in equilibrium with  $CO_2$ , the  
131 following system of reactions is established:



134 The solubility of  $CO_2$  in water depends on the  $CO_2$  partial pressure and on the  
135 system temperature. In an aqueous solution, the speciation of  $CO_2$  depends on the  
136 pH: at a low pH value, the equilibrium shifts towards  $H_2CO_3$  to reduce the  
137 concentration of  $H^+$ , while under basic conditions, the equilibrium promotes more  
138 dissolution of  $H_2CO_3$  to produce  $H^+$  (Pan et al., 2012). This step can be limited due to  
139 poor mixing between the atmospheric  $CO_2$  and the solution, slow transfer of  $CO_2$  from

140 the gas phase to the liquid phase and slow CO<sub>2</sub> hydration (Power et al., 2013; Stumm  
141 and Morgan, 1996; Wilson et al., 2011).

142 The production of H<sup>+</sup> promotes silicate dissolution as shown in equation 3 in  
143 which M can be Ca or Mg (Daval et al., 2009):

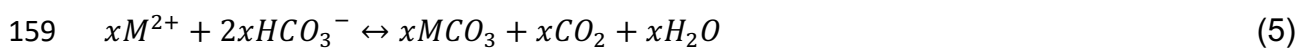


145 Several studies have identified the dissolution of minerals to be the rate-limiting step  
146 in mineral carbonation (e.g., (Daval et al. (2009) and Pullin et al., (2019)). The  
147 dissolution of a mineral depends on the chemical structure of the mineral itself.  
148 Dissolution of minerals such as brucite proceeds faster than the dissolution of  
149 serpentine since brucite dissolution requires breaking a single type of bonds, while the  
150 dissolution of silicate-rich minerals requires breaking of several strong Si-O bonds  
151 (Power et al., 2013; Schott et al., 2009). Consequently, the dissolution of silicate-rich  
152 minerals may proceed non-stoichiometrically, leaving behind a silicon-rich passivating  
153 layer, as described by Schott et al. (2012), Power et al. (2013) and the references  
154 therein.

155 This dissolution reaction is then followed by precipitations reactions as shown in  
156 equations 4 and 5 (Daval et al., 2009):



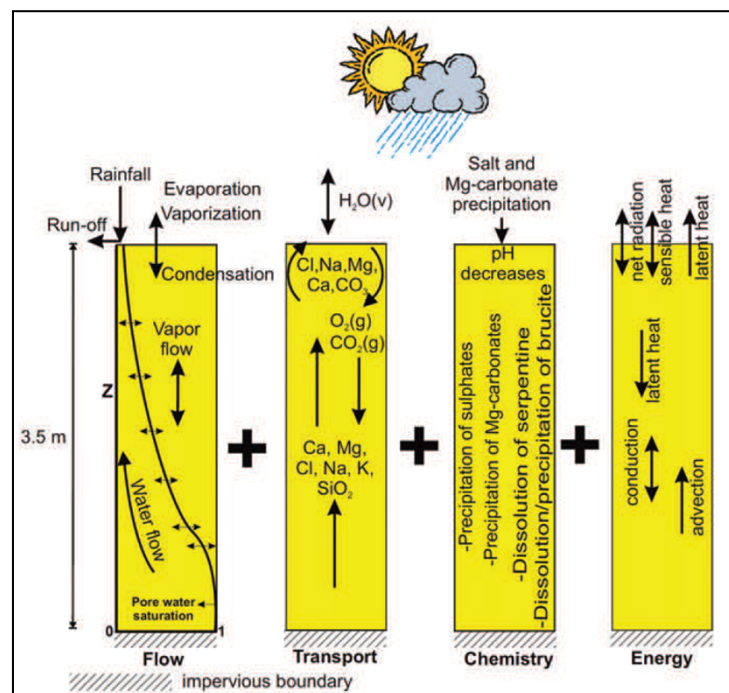
158 Or



## 160 **2.2 Reaction parameters**

161 Due to the huge variation in the chemical and physical properties of alkaline  
162 wastes, and due to the different reactions involved in mineral carbonation, optimizing  
163 CO<sub>2</sub> uptake requires finding the optimum conditions that enhance the steps of the  
164 carbonation reaction. For example, pH has variable effects on the carbonation

165 process. Lower pH increases metal leaching thereby increases the reactants'  
 166 concentrations while higher pH promotes carbonates precipitation (Azdarpour et al.,  
 167 2015; Chen et al., 2019). While increasing the temperature is associated with  
 168 decreased CO<sub>2</sub> solubility in the aqueous solution (Huijgen et al., 2005), increasing the  
 169 temperature from 10 °C to 40 °C was found to positively correlate with cations release  
 170 from alkaline wastes, and the decreased solubility of CO<sub>2</sub> did not represent a limiting  
 171 step (Assima et al., 2014a, 2014b). Increasing the CO<sub>2</sub> partial pressure has also been  
 172 found to increase the carbonation as it enhances mineral dissolution and promotes  
 173 carbonate mineral precipitation (Harrison et al., 2012; Pokrovsky and Schott, 2000).  
 174 Additionally, climate conditions and atmospheric CO<sub>2</sub> concentration can affect the CO<sub>2</sub>  
 175 uptake (Fig. 2). Due to the variations in carbonation mechanism and extent due to the  
 176 chemical and physical variation of alkaline wastes, the quantification of the CO<sub>2</sub> uptake  
 177 relies on combining information obtained from several analysis techniques, some of  
 178 which are portrayed in Table 1.



179

180 Fig. 2. Demonstration of interacting processes that affect CO<sub>2</sub> uptake in alkaline wastes in an arid  
 181 environment. Reprinted from (Bea et al., 2012). Copyright (2012) with permission from Soil Science  
 182 Society of America, Inc.

183

Table 1. Common analysis tools used in studying mineral carbonation of alkaline wastes

Method	Used for	Remarks	Reference
Thermogravimetric Analysis (TGA)	Study dehydroxylation of serpentine and minerals formation/recrystallization. Finding the weight fraction of CaCO <sub>3</sub> in a sample as it decomposes at a certain temperature range (500-1000 °C)	TGA cannot be used for quantification of different mineral phases within a sample. Thermal treatment of serpentine can increase the Mg released for carbonation. However, over heating should be avoided to avoid recrystallisation and production of less reactive minerals.	(Chiang and Pan, 2017; Dlugogorski and Balucan, 2014; Huijgen et al., 2005)
X-ray diffraction (XRD)	Qualitative/quantitative identification of mineral phases.	XRD can distinguish authigenic and pre-existing carbonates. Quantification of different phases in a semi-crystalline sample requires complicated methods such as Rietveld refinements.	(Wilson et al., 2009b, 2006)
Scanning electron microscopy (SEM)	Visualization of microstructures. Observing morphological changes upon carbonation. Identifying composition and mineral phases.	SEM imaging can be used to identify biological mineralisation of carbonates.	(McCutcheon et al., 2017; UI-Hamid, 2018)
Total carbon/ organic carbon (TC/TOC)	Quantifying the amount of carbon within a sample	TOC/ TIC cannot distinguish between authigenic and pre-existing carbonates	(Dembicki, Jr., 2017; LECO Corporation, 2008)
X-ray computed tomography (XCT)	Observing the internal structures and morphology. Quantification and classification in 3D and 4D of mineral phases, porosity and pore connectivity, as well as individual grain analyses (shape, orientation, equivalent diameter, and so on).	XCT is suitable for studying in-situ carbonation. Geometry derived from XCT can be used as input for permeability modelling.	(Baker et al., 2012; Boone et al., 2014)
Stable isotope analysis	Quantify the origin of carbon in a sample (organic, lithogenic, atmospheric)	Stable isotope analysis can be corroborated with radiocarbon analysis to provide evidence of atmospheric CO <sub>2</sub> sequestration	(Renforth, 2011; Washbourne et al., 2012)

184

### 185 **3. Studies of alkaline wastes carbonation**

#### 186 **3.1 Iron and steel slag**

187 The importance of steel in the global economy is evident from the production of  
188 over 3500 types of steel that are consumed in many industries, ranging from simple  
189 cooking equipment to spacecraft (Lai et al., 2012; World Steel Association, 2021). In  
190 2017, it was estimated that for every 1000 kg of steel produced, around 1830 kg CO<sub>2</sub>  
191 is emitted, making this high emission the “biggest challenge” to this industry, as  
192 described by the World Steel Association (World Steel Association, 2019). The  
193 production of 1000 kg of steel results in around 200-400 kg slag, depending on the  
194 mode of production (World Steel Association, 2017). Recently, attempts have been  
195 made to utilize slag in sustainable cement and concrete manufacturing since using it  
196 as aggregate can decrease energy consumptions and emissions associated with  
197 concrete industries, without compromising the mechanical properties of products  
198 (Gencel et al., 2021). Experimentally, it was shown that the carbonation of slag can  
199 produce building materials with compressive strength that increase with increased  
200 CO<sub>2</sub> uptake (Wang et al., 2019).

201 As the United Kingdom (UK) has a rich history in iron and steel production, over  
202  $1.90 \times 10^{11}$  kg of slag deposits exist in the country, providing excellent opportunities for  
203 studying passive carbonation within these alkaline wastes (Riley et al., 2020).  
204 Chukwuma et al. (2021) studied the weathering of iron and steel slag deposits in South  
205 Wales, UK which are associated with iron and steel production that ceased in 1980.  
206 These deposits contain calcium-silicate minerals, dominated by gehlenite  
207 (Ca<sub>2</sub>Al<sub>2</sub>SiO<sub>2</sub>) and åkermanite (Ca<sub>2</sub>MgSi<sub>2</sub>O<sub>2</sub>). Across the studied sites, the stored CO<sub>2</sub>  
208 in the slag was found to reach 66 kg CO<sub>2</sub>/ 1000 kg slag. The carbon capture potential

209 can be estimated based on chemical compositions according to Steinour's formula  
 210 (Gunning et al., 2010; Renforth, 2019):

$$211 \quad C_{pot} = \frac{MW_{CO_2}}{100} \left( \alpha \frac{CaO}{MW_{CaO}} + \beta \frac{MgO}{MW_{MgO}} + \gamma \frac{SO_3}{MW_{SO_3}} + \delta \frac{P_2O_5}{MW_{P_2O_5}} \right) \times 1000 \quad (6)$$

212 Where  $C_{pot}$  refers to the carbonation potential (kg CO<sub>2</sub> uptake/1000 kg wastes), CaO,  
 213 MgO, SO<sub>3</sub> and P<sub>2</sub>O<sub>5</sub> refer to the percentages of the corresponding compounds, MW  
 214 refers to the molar mass, and the coefficients  $\alpha$ ,  $\beta$ ,  $\gamma$ ,  $\delta$  consider the contribution of  
 215 different compounds and they are 1, 1, -1, -2, respectively (Chukwuma et al., 2021).  
 216 Consequently, the maximum measured CO<sub>2</sub> uptake was found to reach 77% of the  
 217 total carbonation potential.

218 Weathering of slag deposits at Consett, UK, provides another example of  
 219 passive CCS (Mayes et al., 2018). These  $2 \times 10^{10}$  kg deposits were produced over  
 220 100 years of operation (ended in 1980) of the Consett Iron and Steel Works that  
 221 produced around  $1.2 \times 10^{11}$  kg of iron and steel (Mayes et al., 2018). XRD analysis  
 222 revealed that the slag was dominated by melilite minerals, and that the downstream  
 223 precipitate is almost entirely composed of calcite (Mayes et al., 2018; Pullin et al.,  
 224 2019). By referring to slag density and chemical compositions, the largest heap was  
 225 estimated to have the potential to sequester  $6 \times 10^9$ - $1.1 \times 10^{10}$  kg CO<sub>2</sub> through mineral  
 226 carbonation (Mayes et al., 2018). However, based on the draining water chemistry and  
 227 calcium leaching and calcite precipitation rates, between  $2.81 \times 10^5$  and  $2.89 \times 10^6$  kg  
 228 CO<sub>2</sub> has been sequestered since 1980, due to the limited inflow of CO<sub>2</sub> into the heap  
 229 and due to the surface passivation of slag with carbonate (Mayes et al., 2018). This  
 230 site was further studied by Pullin et al. (2019) after *Geosonic Drilling Company* drilled  
 231 three boreholes across a 60 m transect. CO<sub>2</sub> concentrations in the boreholes were  
 232 almost 85 ppm, while they reached almost 403 ppm at the surface, reflecting that the  
 233 produced slag has had little interaction with the atmospheric CO<sub>2</sub> (Pullin et al., 2019).

234 With total carbon concentration of 0.42%, Pullin et al. (2019) estimated that only ~ 3%  
235 of CO<sub>2</sub> capture potential was utilized.

236 The production of 1000 kg of steel generates 400 kg of slag and emits 1830 kg  
237 of CO<sub>2</sub> (World Steel Association, 2019, 2017), The previous studies demonstrate that  
238 CO<sub>2</sub> can be passively sequestered within slag. The maximum theoretical CO<sub>2</sub> uptake  
239 in slag is controlled by slag composition and is dictated by CaO and MgO content  
240 (Mayes et al., 2018). With CaO and MgO concentrations vary from 29% to 44% and  
241 5% to 12% respectively (Proctor et al., 2000), it is possible to calculate that utilizing  
242 slag can sequester 113-190 kg CO<sub>2</sub>, or ~10% of CO<sub>2</sub> emitted from the production of  
243 1000 kg of steel, based on the complete conversion of CaO and MgO. However, as  
244 depicted earlier, the CO<sub>2</sub> uptake is much less than the maximum theoretical CO<sub>2</sub>  
245 uptake due to several factors. Ca and Mg are usually incorporated into more complex  
246 mineral structures (Yildirim and Prezzi, 2015). Several slag-forming minerals have  
247 been identified in the literature, and these minerals have variable carbonation rates  
248 (Bodor et al., 2013). These minerals are produced during slag cooling and their  
249 presence is affected by the waste management practice. For example, the cooling rate  
250 has been determined to result in different mineral compositions in slag (Kriskova et  
251 al., 2013). Rapid cooling produces more reactive slag composed of tricalcium silicates  
252 while slow cooling produces åkermanite or gehlenite phases that are less reactive  
253 (Engström et al., 2013; Pullin et al., 2019; Scott et al., 1986). Another issue that  
254 reduces the CO<sub>2</sub> uptake in slag is that slag may be produced at gravel size causing it  
255 to have a low surface area thereby lowering its CO<sub>2</sub> uptake rate (Ragipani et al., 2021).

### 256 **3.2 Demolition wastes in artificial soil**

257 Artificial soils in urban and brownfield land originate from demolition and  
258 construction wastes and provide an opportunity for CCS as they are rich in Ca- and

259 Mg-silicates. These compounds can interact with carbon which originates from the  
260 dissolution of CO<sub>2</sub> from plant respiration and decomposition, or from CO<sub>2</sub> dissolving in  
261 alkaline water, to produce carbonates (Renforth, 2011). This section reviews studies  
262 that investigate the applicability of artificial soils and demolition wastes in CCS  
263 applications.

264 Jorat et al. (2020) investigated soil carbonation in over 20 brownfield sites  
265 across the UK by calculating soil carbonation rates and observing carbonation effects  
266 on permeability and ground strength. Carbonation rate was measured through TIC  
267 measurement of soil to a depth of 20 cm and presented as a function of site age, where  
268 the latter was defined as the period between the demolition and the sampling dates.  
269 Throughout the study period, sites aged between 7 and 26 years had no significant  
270 change in TIC, while there was a statistically significant increase in TIC for three young  
271 sites aged between 2 and 8 years (Jorat et al., 2020). Carbon sequestration occurred  
272 at a rate of 100-1600 g C m<sup>-2</sup> y<sup>-1</sup>, indicating that the higher carbonation rate occurred  
273 at more modern sites as they were more suitable for carbonation, possibly due to their  
274 inclusion of more fine-grained crushed concrete (Jorat et al., 2020).

275 The Science Central Park in Newcastle, UK, has been the subject of passive  
276 carbonation studies (Washbourne et al., 2012, 2015). The 10<sup>5</sup> m<sup>2</sup> site is made up of a  
277 0.2-6 m thick layer of made ground, which contains crushed concrete and aggregate.  
278 Washbourne et al. (2015) studied soil carbonation at this site for 18 months. Over the  
279 study period, the CaCO<sub>3</sub> content within the top 100 mm of the soil increased from 5.3-  
280 43 wt % CaCO<sub>3</sub> to 26.5-61.4 wt% CaCO<sub>3</sub>, where the ranges reflect the content at  
281 different locations within the study site (Washbourne et al., 2015). CaCO<sub>3</sub> content did  
282 not vary with depth in a consistent manner, although it was observed that for some  
283 pits the concentration was larger at shallow depths of less than 1 m, and a decline was



284 observed when the depth exceeded one meter (Washbourne et al., 2015). During the  
285 18-month study period, CO<sub>2</sub> was sequestered at a rate of 2320 g C m<sup>-2</sup> y<sup>-1</sup> with calcite  
286 being the dominant phase of CaCO<sub>3</sub> (Washbourne et al., 2015).

287 Based on the estimations of Renforth et al. (2009) and the references therein,  
288 brownfields occupy 1.45 x 10<sup>10</sup> m<sup>2</sup> globally. With a measured CO<sub>2</sub> uptake of 30 ± 15.3  
289 kg C m<sup>-2</sup>, it can be estimated that brownfields have already captured 4.353 x 10<sup>11</sup> kg  
290 C (Renforth et al., 2009). The annual concrete wastes production reaches 6.8 x 10<sup>12</sup>  
291 kg y<sup>-1</sup>, and it has a maximum carbon capture potential of 2.9 x 10<sup>11</sup> kg C y<sup>-1</sup>, assuming  
292 it contains 20% CaO (Renforth et al., 2009). However, achieving high CO<sub>2</sub> uptake in  
293 demolition wastes is usually challenged by several factors. After the service life of a  
294 structure, it is destructed to produce concrete rubble which is then crushed and  
295 stockpiled for a period between 2 weeks and 4 months (Pade and Guimaraes, 2007).  
296 Importantly, the size of demolition waste materials is a critical factor in their CO<sub>2</sub>  
297 uptake, with sizes larger than 40 mm were found to be unsuitable for carbonation  
298 (Butera et al., 2015). While CO<sub>2</sub> uptake in concrete aggregate increases after  
299 demolition as a result of pulverization, it is also affected by the end use of the  
300 pulverized concrete. Crushed concrete in most countries is used in the manufacturing  
301 of roads and other below-ground applications, thereby reducing its CO<sub>2</sub> uptake  
302 (Marinković et al., 2014; Pade and Guimaraes, 2007).

### 303 **3.3 Mine tailings**

304 Modern industry consumes high quantities of metals, making mining operations  
305 pivotal in economic development. According to the Mining, Minerals and Sustainable  
306 Development (MMSD) Project, there are more than 3500 active mining waste facilities  
307 globally (Tayebi-Khorami et al., 2019), resulting in producing mine wastes at a rate of  
308 2 x 10<sup>12</sup> - 6.5 x 10<sup>12</sup> kg y<sup>-1</sup> (Renforth et al., 2011), and Power et al. (2013) estimated

309 that around  $4.19 \times 10^{11}$  kg of mafic and ultramafic wastes are produced annually.  
310 Mineral compositions of tailings allow them to sequester CO<sub>2</sub> and offset emissions  
311 from mining industries. The carbonation capacity of tailings is associated with the  
312 complete conversion of their Ca and Mg to carbonates on a mole per mole basis (Paulo  
313 et al., 2021). Several minerals, such as brucite, lizardite, diopside, forsterite and  
314 wollastonite have been identified as possible sources for cations although these  
315 minerals have different dissolution rates. Brucite has the highest dissolution rate  
316 across a wide range of pH values that is orders of magnitude larger than that of Mg-  
317 silicate minerals (Power et al., 2013). Nevertheless, other silicate minerals such as  
318 serpentine provide significant CO<sub>2</sub> uptake capacity as they release magnesium that is  
319 loosely bound to the silicate surface (Assima et al., 2013; Stubbs et al., 2022;  
320 Vanderzee et al., 2019).

### 321 **3.3.1 Nickel mining**

322 Passive carbonation of mine tailings and waste rocks associated with nickel  
323 mining operations in Québec, Canada has been the subject of some studies (Gras et  
324 al., 2020, 2017, 2015). The CO<sub>2</sub> uptake by these wastes was estimated by following  
325 the carbonation over a 4-year period using two different setups: the first one, referred  
326 to as EC-1 cell, contained  $1.04 \times 10^5$  kg of heterogeneous waste rocks, ranging from  
327 block to silt size, and a second cell, referred to EC-2 cell, contained  $\sim 2.1$  m<sup>3</sup> of mine  
328 tailings (Gras et al., 2017). The dominant mineral phases were chrysotile, lizardite,  
329 brucite and magnetite, while minor amounts of calcite and millerite were present (Gras  
330 et al., 2017; Pronost et al., 2010). Upon weathering, crusts formed on the surface of  
331 most rock fragments in EC-1 and near the edges of the tailings in EC-2 (Gras et al.,  
332 2017). In both cells, the CO<sub>2</sub> concentration decreased from the atmospheric value of  
333 390 ppmv at the surface, to 50 ppmv and 25 ppmv in EC-1 and EC-2, respectively,

334 and the CO<sub>2</sub> drop increased as the depth increased. CO<sub>2</sub> concentration within both  
335 cells increased from year to year and this increase was accompanied by a reduction  
336 of brucite peak in the XRD analysis and an increase in carbonate minerals. Therefore,  
337 the reduction of the carbon capture rate was attributed to the consumption of the  
338 brucite or the surface passivation due to the formation of carbonate (Gras et al., 2017).

339 Wastes from nickel mining were also investigated to quantify the carbonation  
340 process in Mount Keith, Western Australia (Wilson et al., 2014). XRD analysis of  
341 several samples collected from the tailing facilities showed that the majority of minerals  
342 were serpentines, including antigorite and lizardite, and hydrotalcite minerals,  
343 including iowate and woodalite. There were also minor amounts of brucite, chrysotile,  
344 calcite and dolomite. Efflorescence was spotted at the surface of the tailings, and it  
345 was dominated by hydromagnesite, halite and hexahydrate. Hydromagnesite was also  
346 detected in most of the collected samples, and its highest presence was recorded at  
347 shallow depths, mostly filling cracks and fissures of serpentine or on the surface of  
348 serpentine grains. The abundance of brucite/serpentine decreased with time, while the  
349 amount of hydromagnesite increased (Wilson et al., 2014). The greatest amount of  
350 hydromagnesite was recorded in the top 25 cm of the tailings, coinciding with the  
351 lowest amount of serpentine and brucite. Current rates of passive carbon  
352 mineralization offset ~11% of greenhouse gases emitted from Mount Keith mine, and  
353 enhancing carbon mineralization to carbonate the brucite alone will result in offsetting  
354 the CO<sub>2</sub> emissions from Mount Keith mining by at least 20% (Harrison et al., 2012;  
355 Wilson et al., 2014).

### 356 **3.3.2 Chrysotile mining**

357 Due to the health problems of asbestos, chrysotile mining has significantly  
358 decreased (World Health Organization, 2014). However, there are several chrysotile

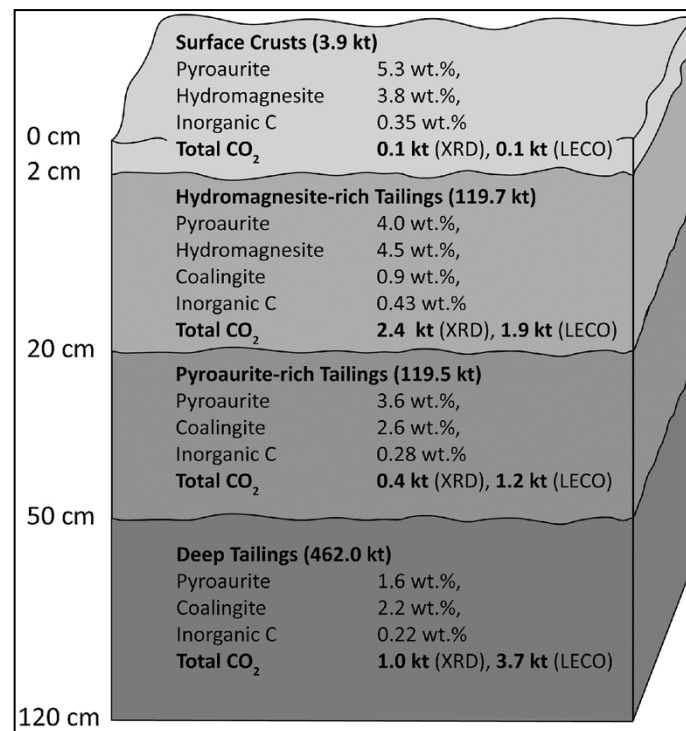
359 tailings sites that provide excellent opportunities to study and quantify mineral  
360 carbonation within chrysotile tailings. For example, Clinton creek in Yukon Territory,  
361 Canada hosts  $1 \times 10^{10}$  kg of tailings (Indian and Northern Affairs Canada, 2008; Wilson  
362 et al., 2009a). Nesquehonite was observed to form towards the surface of the tailings  
363 as a result of evaporative precipitation, while dypingite and hydromagnesite were  
364 observed to cement serpentine grains below the nesquehonite-covered surfaces, or  
365 on the surface of cobbles. High  $\text{CO}_2$  uptake of  $1.64 \times 10^8$  kg was calculated,  
366 corresponding to  $6.3 \times 10^6$  kg  $\text{CO}_2 \text{ y}^{-1}$  when considering the age of 26 years (Wilson  
367 et al., 2009a, 2006).

368 Oskierski et al. (2013) investigated the carbonation potential of chrysotile mine  
369 tailings within Woodsreef asbestos mine in Australia, where mining took place  
370 between 1906 and 1983, producing about  $5.5 \times 10^8$  kg of fibers from  $2.5 \times 10^{10}$  kg ore,  
371 most of which was produced between 1971 and 1983 (Brown et al., 1992; Oskierski  
372 et al., 2013). At the studied location, there were several modes of carbonate  
373 occurrence, including horizontal and vertical crusts. Crust samples were analyzed  
374 through XRD analysis which revealed the predominance of serpentine minerals  
375 (Oskierski et al., 2013). Brucite and carbonate minerals, such as hydromagnesite,  
376 pyroaurite, calcite, dolomite and magnesite, were present at varying amounts. Around  
377  $1.4 \times 10^6$  kg of  $\text{CO}_2$  are stored within the crusts, providing a lower estimate of the  
378 carbonation (Oskierski et al., 2013). An upper estimate of  $7.0 \times 10^7$  kg  $\text{CO}_2$  can be  
379 calculated if pyroaurite, which was estimated to have a concentration of 4.3 wt% within  
380 the tailings pile, is also considered as product of mineral carbonation. Considering that  
381 carbonation has occurred since the closure of the mine over a period of 29 years, the  
382 carbonation rate was calculated to be between  $27 \text{ g C m}^{-2} \text{ y}^{-1}$  and  $1330 \text{ g C m}^{-2} \text{ y}^{-1}$   
383 (Oskierski et al., 2013). Oskierski et al. (2016) highlighted the importance of

384 evaporation in carbonate precipitation, as evident from the high  $\delta^{18}\text{O}$  signature in the  
385 precipitated hydromagnesite, and the high values of  $\delta^{13}\text{C}$  that was associated with  
386 evaporative enrichment prior to precipitation (Oskierski et al., 2021, 2016).

387 Woodsreef mine wastes were further studied in later research which  
388 investigated the mineral composition of the top 120 cm of the mine wastes (Turvey et  
389 al., 2018b). The amount of captured  $\text{CO}_2$  was estimated using two different  
390 approaches: i) quantitative XRD, where the mineral composition was estimated using  
391 structureless fitting methods, as explained elsewhere (Turvey et al., 2018b, 2018a,  
392 2017) and the references therein; ii) and by measuring the total elemental carbon and  
393 then finding the inorganic carbon by assuming an average value of the organic carbon  
394 to be 0.02 wt % C as suggested in the literature (Hamilton et al., n.d.; Turvey et al.,  
395 2018b). XRD data demonstrated that the presence of several forms of carbonates  
396 varied with depth. To provide conservative estimates of carbonation rates, it was  
397 assumed that carbon sequestration occurred within the top 120 cm of the tailing. XRD  
398 analysis showed that there were different modes of carbonation occurring within the  
399 study region: in the shallow depths (up to 40 cm),  $\text{CO}_2$  sequestration occurred as a  
400 result of brucite carbonation that produces hydromagnesite. On the other hand, at  
401 larger depth where  $\text{CO}_2$  supply is limited, coalingite and pyroaurite were the primary  
402 carbonation products, as portrayed in Fig. 3. The carbon content based on XRD data  
403 and elemental carbon measurement through the studied region was found to be  $3.9 \times$   
404  $10^6$  kg  $\text{CO}_2$  and  $6.9 \times 10^6$  kg  $\text{CO}_2$ , respectively. The value obtained from the XRD  
405 provides a lower estimate, since XRD analysis does not take into account the carbon  
406 that resides in amorphous structures, and the quantification method was shown to  
407 underestimate the amount of carbonates within tailings (Turvey et al., 2018a). On the  
408 other hand, as the elemental carbon data report the total carbon content, without

409 restricting the amount of carbon to the minerals that were produced as a result of CO<sub>2</sub>  
 410 sequestration, the obtained value reflected the upper estimates of the CO<sub>2</sub>  
 411 sequestration at Woodsreef. Considering these end members, the carbonation  
 412 potential was estimated to be between 62 and 110 g C m<sup>-2</sup> y<sup>-1</sup>, a range that overlaps  
 413 with the carbonation range reported by Oskierski et al. (2013). Turvey et al. (2018b)  
 414 attributed this to the fact that Oskierski et al. (2013) estimated that pyroaurite has a  
 415 concentration of 4.3%, which was proven to be not the case, as shown in Fig. 3. More  
 416 representative values of CO<sub>2</sub> sequestration can be obtained by obtaining mineralogical  
 417 composition and carbon content at higher depth within tailings.



418

419 Fig. 3. Variation in mineralogical composition and CO<sub>2</sub> sequestration with depth at Woodsreef mine  
 420 tailings. Values next to XRD represent the amount of CO<sub>2</sub> sequestered as estimated using XRD  
 421 analysis while values next to LECO represent the amount of CO<sub>2</sub> sequestered as estimated using  
 422 total elemental carbon. Reprinted from (Turvey et al., 2018b), Copyright (2018) with permission from  
 423 Elsevier.

### 424 3.3.3 Kimberlite mining

425 Kimberlites are volatile-rich, ultramafic rocks that are being mined for diamonds.  
 426 (Mitchel, 1986; Wilson et al., 2011). There is some evidence that processed kimberlite

427 can sequester atmospheric CO<sub>2</sub>. For example, it was estimated that around 1.8 x 10<sup>6</sup>  
428 kg CO<sub>2</sub> may have been sequestered in the processed kimberlite at the Diavik diamond  
429 mine in the Canadian northwestern territories (Wilson et al., 2009b). At Diavik, the  
430 processed kimberlite contained serpentine minerals, forsterite and minor amounts of  
431 other minerals, including clay minerals, Mg-rich garnet and plagioclase feldspar  
432 (Wilson et al., 2011, 2009b). Nesquehonite was the most common form of secondary  
433 carbonates, taking the shape of continuous films at the surface of the tailings. Wilson  
434 et al. (2011) reported that nesquehonite formed on the surface of forsterite and  
435 serpentine, indicating that it precipitated due to mineral weathering, resulting in  
436 trapping of carbon at a rate of 102-114 g C m<sup>-2</sup> y<sup>-1</sup>, which is two orders of magnitude  
437 higher than natural silicate weathering in river catchments in areas with similar climatic  
438 conditions (Huh, 2003; Wilson et al., 2011). The waste management practice, in which  
439 the tailings are stored under process water, severely limits the carbonation rate  
440 (Wilson et al., 2011, 2009b).

441 Mervine et al. (2018) studied the carbonation potential of processed kimberlite  
442 in different mines in Canada and in South Africa. Several minerals with high  
443 carbonation potentials were detected, including serpentine, olivine, brucite, and  
444 smectite. Serpentine was the most abundant mineral, having the bulk of CO<sub>2</sub> capture  
445 potential associated with its high content of labile Mg<sup>2+</sup> (Mervine et al., 2018; Stubbs  
446 et al., 2022; Vanderzee et al., 2019). Although present at a small fraction, brucite is  
447 important as it can be carbonated at relatively low temperature and pressure. Different  
448 forms of carbonates, including calcite, dolomite, magnesite and siderite were detected  
449 at variable concentrations. Using the mineral and chemical properties of the kimberlite  
450 and carbonation potential correlation published elsewhere (Wilson et al., 2009b), it  
451 was estimated that carbonation of 4.7 to 24 wt% of the annual processed kimberlite

452 can result in offsetting 100% of CO<sub>2</sub> equivalent emitted from each mining site (Mervine  
453 et al., 2018).

#### 454 **3.3.4 Red mud**

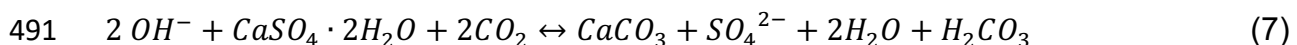
455 Red mud is produced from bauxite/aluminum ore processing. Due to its  
456 physical and chemical properties, notably ductility and malleability, aluminum is the  
457 most used metal after iron and steel (Geoscience Australia, 2018). Red mud is  
458 produced at a rate of 1-1.5 kg per kg of produced alumina (Al<sub>2</sub>O<sub>3</sub>) (Yang and Xiao,  
459 2008), resulting in a world stock of ~4 x 10<sup>12</sup> kg in 2015 (Gore, 2015; Mukiza et al.,  
460 2019). Most of today's alumina is produced through the Bayer process, which involves  
461 mixing the finely ground ore with caustic soda (Geoscience Australia, 2018). The  
462 produced alumina is in turn smelted through the Hall-Héroult smelting process to  
463 produce aluminum (Geoscience Australia, 2018). The by-product residue is thickened  
464 in a process known as dry stacking. Mixing the residue with CO<sub>2</sub> can reduce the pH of  
465 the suspension from 13 to less than 10.5, making the slurry more suitable for biological  
466 activities that promote the breakdown down of organic residues. Residue carbonation  
467 has been found to enhance drying rates, requiring less area thereby resulting in  
468 aesthetic and cost benefits (Alcoa, 2012).

469 Red mud has a potential to passively sequester CO<sub>2</sub> at ambient conditions. Si  
470 et al. (2013) investigated the carbonation potential of different red mud residues that  
471 were collected from different aluminum refineries in China and Australia. They  
472 calculated the maximum carbonation potential (which they defined as the total  
473 alkalinity of red mud, assuming that 2 moles of OH<sup>-</sup> can capture 1 mole of CO<sub>2</sub>) and  
474 actual carbonation (defined as total carbon concentration of red mud) and revealed  
475 that the maximum carbonation significantly exceeds the actual carbonation by up to  
476 more than 100%. This was attributed to the treatment of red mud with seawater, which



477 removes a considerable amount of alkali metals that could have been utilized in  
478 carbonation. Additionally, XRD analysis detected perovskite and larnite, indicating that  
479  $\text{TiO}_3^{2-}$  and  $\text{SiO}_4^{2-}$  compete with carbonate for  $\text{Ca}^{2+}$ . Based on the current red mud  
480 production rate of  $1.2 \times 10^{11} \text{ kg y}^{-1}$  (Power et al., 2011) and based on the estimated  
481  $\text{CO}_2$  uptake of 15 kg C / 1000 kg red mud, Si et al. (2013) estimated that approximately  
482  $6 \times 10^9$  kg of  $\text{CO}_2$  can be sequestered within red mud annually, and another  $6 \times 10^9$  kg  
483  $\text{CO}_2$  can be sequestered if adequate technologies (such as supplying of  $\text{Ca}^{2+}$ ) are  
484 used.

485 Renforth et al. (2012) investigated the accidental release of a high quantity ( $6 \times$   
486  $10^5 - 7 \times 10^5 \text{ m}^3$ ) of hyper alkaline (pH= 13) red mud in Ajka, western Hungary (Urbán  
487 and Cséplı, 2010). Atmospheric  $\text{CO}_2$  readily ingresses in such hyperalkaline solutions.  
488 As a mitigation strategy, gypsum was added since it provides a source of  $\text{Ca}^{2+}$  and  
489 result in precipitation of calcium carbonate resulting in decreasing the pH, as show in  
490 equation 7:



492 Based on carbonate, elements, and stable isotope analysis, it was shown that  
493 high sulfur content was strongly correlated with high atmospheric  $\text{CO}_2$  sequestration.  
494 It was calculated that mixing 1000 kg of red mud with 860 kg of gypsum can result in  
495 sequestration of 220 kg  $\text{CO}_2$ . With the figures of gypsum and red mud production rates  
496 that are reported in Renforth et al. (2012) and the references therein, it was estimated  
497 that red mud carbonation through gypsum addition can sequester around  $1.3 \times 10^{10} -$   
498  $2.6 \times 10^{10}$  kg  $\text{CO}_2$  which corresponds to 3 - 4% of  $\text{CO}_2$  emitted from primary production  
499 of aluminum (Harnisch et al., 1998; Renforth et al., 2012).

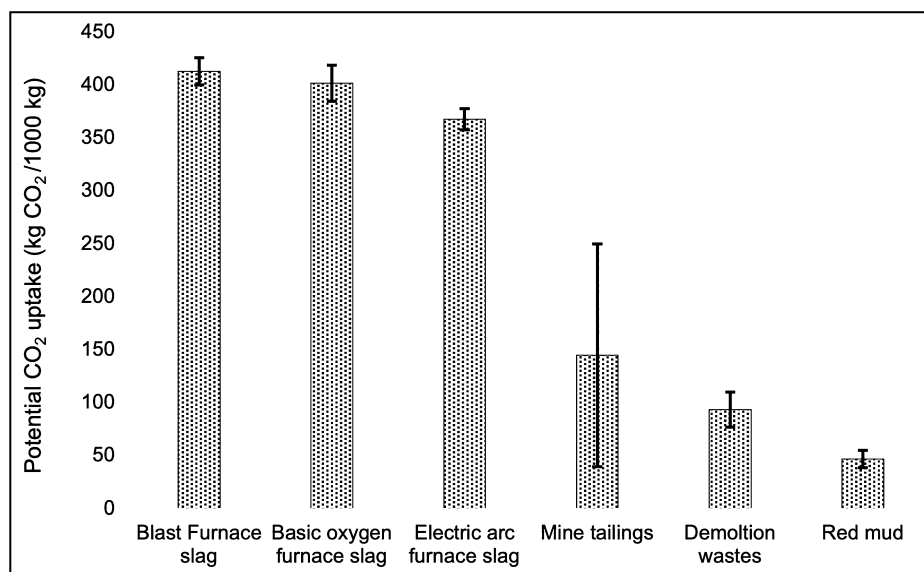
500 The idea of adding  $\text{Ca}^{2+}$  sources to neutralize alkaline red mud was also  
501 investigated by Han et al. (2017). Particularly, the effect of adding gypsum or calcium

502 chloride on enhancing the sequestration potential of bauxite residue and on the pH  
503 reduction was studied on two scales: 55-day batch tests, during which the pH values  
504 of slurry solutions were reduced using atmospheric CO<sub>2</sub> at ambient conditions, and  
505 field neutralization tests, during which 100 kg of bauxite was distributed over a 4 m<sup>2</sup>  
506 area for 120 days. Batch tests demonstrated that carbonation decreased pH to 9.5  
507 (bauxite residue), indicating consumption of pore water alkalinity. The addition of Ca<sup>2+</sup>  
508 sources decreased the pH further, as demonstrated for the gypsum-treated and CaCl<sub>2</sub>-  
509 treated residues, for which the pH dropped to 8.3 and 7.7, respectively. Han et al.  
510 (2017) quantified that it is possible to sequester 0.083 g CO<sub>2</sub> to neutralize 1 g of  
511 bauxite residue, or to 2.3x10<sup>7</sup> kg CO<sub>2</sub> per the 2.8x10<sup>8</sup> kg of bauxite residue produced  
512 in Korea.

513 Another study (Khaitan et al., 2010) investigated simultaneous CO<sub>2</sub>  
514 sequestration and bauxite residue neutralization at two different locations in Texas,  
515 US, namely the Sherwin and Copano bauxite storage facilities, aged 35 and 14 years  
516 at the time of study, respectively. The older site had lower pH; the surface pH at  
517 Sherwin was 9.5, while at Copano it was 10.5. Total carbon was higher at Sherwin  
518 and in both sites, and there was a trend showing that higher carbonation extent  
519 occurred closer to the surface. Moreover, XRD results at Copano showed that a more  
520 pronounced peak of calcite occurred at the surface accompanied by a decrease in  
521 tricalcium aluminate as compared to deeper regions. Atmospheric CO<sub>2</sub> could reduce  
522 the pH of red mud, and the existence of some vegetation such as bitter weed and  
523 Bermuda grass could further reduce the pH to 9, in alignment with increased carbon  
524 content in vegetated locations.

### 525 3.4 Summary: alkaline wastes carbonation potential

526 Annually, around  $7 \times 10^{12}$  kg of silicate wastes are produced on the global scale  
 527 (Renforth et al., 2011). Using Steinour's formula (equation 6), Renforth (2019)  
 528 estimated the carbon capture potential of these wastes, as shown in Fig. 4. Renforth  
 529 (2019) modelled the production of alkaline wastes and their contributions to carbon  
 530 mitigation strategies based on different socioeconomic pathways, which are scenarios  
 531 that enable an analysis of future climate impacts, vulnerabilities, mitigation and  
 532 adaptation based on several drivers, such as urbanization, population and economic  
 533 growth (Riahi et al., 2017). CO<sub>2</sub> emissions are predicted to be between  $2.4 \times 10^{13}$  -  
 534  $1.26 \times 10^{14}$  kg CO<sub>2</sub> y<sup>-1</sup> by 2100, and CO<sub>2</sub> uptake potential within alkaline wastes can  
 535 be between  $2.9 \times 10^{12}$  -  $5.9 \times 10^{12}$  kg CO<sub>2</sub> y<sup>-1</sup>. In other words, alkaline wastes can  
 536 mitigate 5-12 % of CO<sub>2</sub> emissions (Renforth, 2019).



537

538 Fig. 4. CO<sub>2</sub> capture potential of various alkaline wastes. Error bars reflect variation of carbonation  
 539 potentials as a result of different compositions. The figure is based on data from (Renforth, 2019)

540 Clearly, the studied wastes can offset significant amounts of CO<sub>2</sub> emissions.

541 Nevertheless, the CO<sub>2</sub> uptake potential of alkaline wastes can be overestimated. This

542 is because it is calculated based on the conversion of Mg and Ca to carbonate

543 minerals on a mole per mole basis. Paulo et al. (2021) explained that the source of

544 these cations should be considered in the estimation of carbonation capacity, since  
545 these cations may be present in carbonate minerals, and carbonates are an  
546 undesirable source of cations. Consequently, Paulo et al. (2021) suggested a leaching  
547 test that is coupled with a TIC test to identify the cations that reside in carbonates and  
548 to exclude them from carbonation capacity calculations.

549 Table 2 reports the CO<sub>2</sub> uptake at various locations showing. At Mount Keith,  
550 passive sequestration offsets 11% of annual emissions and has carbon capture  
551 potential that exceeds the emissions by a factor of 10 (Wilson et al., 2014). A smaller  
552 offset is observed at Diavik in Canada where the tailings offset 0.2% of the emissions  
553 due to the arid and cold climate in that region and due subaqueous waste storage  
554 (Wilson et al., 2011). Though it is difficult to compare carbonation rates since minerals,  
555 emplacement and climate conditions vary, Table 2 shows that carbonation rates from  
556 reviewed sites are generally in the same order of magnitude, and carbonation occurs  
557 even in subarctic and arid climates. One issue to be addressed is that the reported  
558 CO<sub>2</sub> uptake values are based on different assumptions. For example, the value  
559 provided for Clinton creek was based on two samples: the first sample was assumed  
560 to be representative of 2/3 of the tailings while the second one was assumed to be  
561 representative of 1/3, and the overall CO<sub>2</sub> uptake was estimated based on the  
562 composition of these sample (Wilson et al., 2006). On the other hand, Turvey et al.  
563 (2018b) reported the distribution of the minerals with depth and considered the  
564 incomplete conversion to hydrotalcite minerals in the estimation of carbonation.  
565 Clearly, different methods may result in different estimation of CO<sub>2</sub> uptake in alkaline  
566 wastes.

567

Table 2. CO<sub>2</sub> uptake and the observed carbonates at different sites

Commodity	Location	CO <sub>2</sub> uptake	Observed carbonates	Remarks	Reference
Slag	Consett, UK	7.6x10 <sup>3</sup> -7.8x10 <sup>4</sup> (kg CO <sub>2</sub> /y)	Calcite	δ <sup>13</sup> C, δ <sup>16</sup> O data suggest that between 54% and 99% of the precipitated carbon is from atmospheric origin and the rest is from lithogenic origins.	(Mayes et al., 2018)
Slag	Ohio, United states	0.23 – 3.94 (kg CO <sub>2</sub> /1000 kg slag / y)	Calcite	The slag was used to neutralize acid-mine drainage, and the provided uptake value is based on PHREEQC calculations.	(Goetz and Riefler, 2015)
Demolition wastes	Several towns in England, UK	0.4–5.9 (kg CO <sub>2</sub> /m <sup>2</sup> /y)	Calcite	The largest amount of CO <sub>2</sub> was captured during the first 15 years after demolition. δ <sup>13</sup> C and δ <sup>16</sup> O suggest the removal of CO <sub>2</sub> from the atmosphere via biological and chemical processes.	(Jorat et al., 2020)
Nickel wastes	Dumont, Québec, Canada	0.60-2.2 (kg CO <sub>2</sub> /m <sup>2</sup> /y)	Hydrotalcites, aragonite, nesquehonite, dypingite and hydromagnesite	δ <sup>13</sup> C and δ <sup>16</sup> O suggest precipitation of carbonates under an evaporative environment.	(Gras et al., 2017; Kandji et al., 2017)
Chrysotile wastes	Woodsreef, Australia	0.099- 4.9 (kg CO <sub>2</sub> /m <sup>2</sup> /y)	Hydromagnesite, hydrotalcite, dolomite, calcite, magnesite	High values of δ <sup>13</sup> C, δ <sup>16</sup> O and F14C in hydromagnesite suggest precipitation form atmospheric CO <sub>2</sub> contained in meteoric water. For pyroaurite, the δ <sup>13</sup> C, δ <sup>16</sup> O are close to those of bedrock, although it contained significant radiocarbon.	(Oskierski et al., 2013)
Chrysotile wastes	Woodsreef, Australia	0.229-0.405 (kg CO <sub>2</sub> /m <sup>2</sup> /y)	Hydromagnesite, coalingite and pyroaurite	Availability of CO <sub>2</sub> affect the type of carbonate produced. At a shallow depth, hydromagnesite is produced while at a larger depth, hydrotalcite is produced. Modern atmosphere CO <sub>2</sub> was found to be a source of carbon in the precipitated hydromagnesite and pyroaurite.	(Turvey et al., 2018b)
Chrysotile wastes	Yukon, Clinton creek, Canada	6.2 (kg CO <sub>2</sub> /m <sup>2</sup> /y <sup>1</sup> )	Nesquehonite hydromagnesite, dypingite, lansfordite	Several modes of carbonates were observed, including cements, cobble coatings and crusts. Values of δ <sup>13</sup> C, δ <sup>16</sup> O and F <sup>14</sup> C indicate carbonates formation from modern CO <sub>2</sub> .	(Schuiling et al., 2011; Wilson et al., 2009a)

Chrysotile wastes	Thetford, Québec, Canada	0.98 - 120 (kg CO <sub>2</sub> /m <sup>2</sup> /y)	Hydromagnesite, pyroaurite, sjögrenite	The exothermic CO <sub>2</sub> mineralization reaction resulted in warming the air that vent the surface of chrysotile heap. This warm air is CO <sub>2</sub> depleted, in winter, this air contained 10-18 ppm CO <sub>2</sub> , while in summer it contained 260-370 ppm CO <sub>2</sub>	(Lechat et al., 2016; Pronost et al., 2012)
Kimberlite wastes	Diavik NT, Canada	0.374-0.418 (kg CO <sub>2</sub> /m <sup>2</sup> /y)	Nesquehonite, dolomite, calcite, vaterite, and other Na/Ca bearing carbonates	δ <sup>13</sup> C, δ <sup>16</sup> O and F14C analyses suggested that at least 89% of carbon in secondary carbonates is sourced from the atmosphere either directly or through biological activity.	(Wilson et al., 2011)

## 4. Limitations of passive carbonation

### 4.1 Slow carbonation due to limited CO<sub>2</sub> supply

One of the primary reasons for the low carbonation rate of alkaline wastes is the low concentration of CO<sub>2</sub> in the atmosphere. Passive carbonation relies on using atmospheric air which is ~0.04% CO<sub>2</sub>, causing it to be more difficult when compared to techniques that use a concentrated CO<sub>2</sub> stream (Buis, 2019; Wilcox et al., 2017). Therefore, increasing the exposure of wastes to CO<sub>2</sub> has been suggested as a method to increase CO<sub>2</sub> uptake. In a study that investigated the carbonation of a subarctic chromite mine shaft in Norway, it was noted that air circulation can enhance the carbonation (Beinlich and Austrheim, 2012). For mines that have a single entrance, carbonation was limited near the entry point while for mines that have multiple entrances, air circulation was enhanced and carbonation was observed to occur throughout these mines. Harrison et al. (2012) studied the carbonation of brucite, at conditions that mimic those at Mount Keith nickel mine. They investigated the effect of increasing the CO<sub>2</sub> concentration, under a system pressure of 0.1 MPa, on the carbonation of brucite, and demonstrated that as the concentration of CO<sub>2</sub> increased from 0.04% to 100%, the carbonation rate increased by ~2400 fold. This carbonation rate can offset up to ~57% of CO<sub>2</sub> emissions from Mount Keith nickel mine (Harrison et al., 2012).

Different carbonation products may form in different environments, depending on CO<sub>2</sub> availability. In environments where CO<sub>2</sub> supply is limited, incomplete carbonation can produce hydrotalcite minerals. This was documented at Woodsreef where at shallow depth hydromagnesite (Mg<sub>5</sub>(CO<sub>3</sub>)<sub>4</sub>(OH)<sub>2</sub>·4H<sub>2</sub>O) is produced while hydrotalcite minerals such as pyroaurite (Mg<sub>6</sub>Fe<sub>2</sub><sup>3+</sup>(CO<sub>3</sub>)(OH)<sub>16</sub>·4H<sub>2</sub>O) and coalingite

593  $(\text{Mg}_{10}\text{Fe}_2^{3+}(\text{CO}_3)(\text{OH})_{24}\cdot 2\text{H}_2\text{O})$  are produced at larger depths where  $\text{CO}_2$  supply is  
594 limited (Turvey et al., 2018b). The work of Turvey et al. (2018b) provides evidence that  
595 increasing  $\text{CO}_2$  availability in tailings results in the formation of more efficient  $\text{CO}_2$   
596 sinks that can sequester a higher amount of  $\text{CO}_2$  for a given amount of Mg and result  
597 in a lower volume of precipitated carbonates.

## 598 **4.2 Carbonation reduction due to negative feedbacks**

599 Negative feedback loops can be caused by the carbonation reaction products  
600 which precipitate at or near the reactive sites and thus prevent  $\text{CO}_2$  from reaching  
601 those sites. This behaviour has been reported particularly in ex-situ carbonation  
602 studies. For example, Chang et al. (2012) observed that as pulverized slag ( $<63\ \mu\text{m}$ )  
603 is carbonated, a layer of carbonate forms around the particle, and its thickness  
604 increases as the reaction proceeds, resulting in limiting further carbonation. The  
605 generation of the passivation layer can also result from silanol polymerization. Assima  
606 et al. (2013) investigated this issue by studying  $\text{CO}_2$  uptake in chrysotile mining wastes  
607 that contained different amounts of water. For a given amount of water, Assima et al.  
608 (2013) showed that increasing the watering frequency positively correlated with  
609 increasing  $\text{CO}_2$  uptake. Higher watering frequency resulted in  $\text{Mg}^{2+}$  supersaturation  
610 in pore water and increased its pH, resulting in more carbonate precipitation. When  
611 water was added, it transported the carbonation products to larger depths and allowed  
612 upper pores to host further carbonation reactions. Additionally, it was demonstrated  
613 that the addition of water on episodes reduces surface passivation through silica gel  
614 polymerisation, since polymerisation is promoted when an excess amount of water is  
615 added (Assima et al., 2012; Grénman et al., 2008). It should be noted that carbonation  
616 may be reduced as a result of permeability reduction caused by carbonates  
617 precipitation. However, Assima et al. (2013) observed that when chrysotile wastes



618 interact with CO<sub>2</sub>-lean stream in a saturation-controlled porous bed, the pressure drop  
619 decreased as the carbonation progressed, reflecting that clogging was outpaced by  
620 dissolution.

621 However, it should be noted that volume expansion can cause a positive  
622 feedback, which is explained by a “reaction driven cracking” as explained by Kelemen  
623 et al. (2020) and the references therein. In this process, volume expansion due to the  
624 carbonation causes differential stresses which in turn cause fractures that enhance  
625 the permeability and facilitate delivery of reactants to reactive sites, thereby enhancing  
626 the degree of carbonation as observed in carbonates precipitation in mines walls and  
627 ceilings (Beinlich and Austrheim, 2012). Understanding the chemo-mechanical factors  
628 can help in establishing a phase diagram that elucidates the conditions that promote  
629 positive feedback and carbonation enhancement (Kelemen et al., 2020).

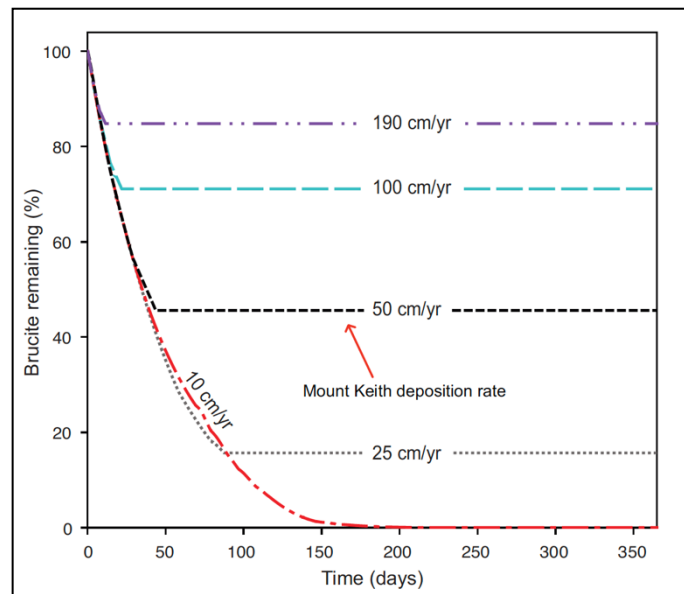
### 630 **4.3 Waste generation and management practice**

631 Alkaline wastes have the potential to sequester  $1.90 \times 10^{11}$  -  $3.32 \times 10^{11}$  kg C y<sup>-1</sup>  
632 (Renforth et al., 2011). Yet this potential is hindered because when tailing storage  
633 facilities were designed, mineral carbonation had not been considered. Waste  
634 management practice can be tailored to favour CCS by enhancing cations leaching  
635 (Power et al., 2014). This can be done through different pathways, for example, by  
636 acidity generation through bioleaching using different kinds of bacteria, such as *L.*  
637 *ferrooxidans*, *A. ferrooxidans* and *A. thiooxidans* (Edwards and Goebel, 1999;  
638 Nordstrom and Southam, 1997; Power et al., 2014). These bacteria decrease the pH  
639 by producing sulfuric acid through bio-oxidation of sulphur that exists within minerals  
640 in copper, uranium and gold ores. Power et al. (2010) reported that the addition of  
641 sulphur (which acts as an acid-generating species) and *A. thiooxidans* to tailings  
642 increased the concentration of magnesium in leachates by an order of magnitude. This

643 magnesium-rich leachate can be transferred to carbonation ponds where  
644 cyanobacteria is added to generate alkalinity and to provide nucleation sites for  
645 carbonate precipitation (McCutcheon et al., 2016; Power et al., 2010).

646         Additionally, passive carbonation can be enhanced by increasing the contact  
647 between tailings and the atmosphere and/or water, whether from meteoric or process  
648 sources (Power et al., 2014). For a given deposition rate, increasing the number of  
649 deposition points results in decreasing the period during which tailing are deposited  
650 over a given area, allowing for a formation of thinner tailings that cover a larger area  
651 (Wilson et al., 2014). At Mount Keith mine, tailings are deposited from nine risers that  
652 are concentrated towards the center of the tailings storage facility. Increasing the  
653 number of risers results in a more thin and uniform distribution of tailings across a  
654 large surface area, allowing for more time for mineral carbonation and CO<sub>2</sub>  
655 sequestration, as was shown through reactive transport modelling done by Wilson et  
656 al. (2014) (Fig. 5). Alternatively, using forced-air systems to enhance air circulation  
657 inside wastes piles has also been suggested, based on numerical modeling that  
658 showed that CO<sub>2</sub> concentration is reduced inside the waste piles since the  
659 mineralization rate is higher than the CO<sub>2</sub> supply rate (Nowamooz et al., 2018). Power  
660 et al. (2014) established a decision tree for choosing a waste management practice,  
661 based on the availability of resources (water, waste organics, and area) and sources  
662 of CO<sub>2</sub>, whether from the atmosphere or a concentrated CO<sub>2</sub> stream, as depicted in  
663 Fig. 6. In Scenario A, low carbon can be enhanced by introducing waste organics or  
664 by increasing the waste deposition area, making this scenario suitable for application  
665 at abandoned sites or away from CO<sub>2</sub> generating sources. Scenario B aims to increase  
666 the concentration Mg<sup>2+</sup> in the presence of a concentrated CO<sub>2</sub> stream, cation  
667 availability limits carbonation (Harrison et al., 2013; Power et al., 2014). Scenario B

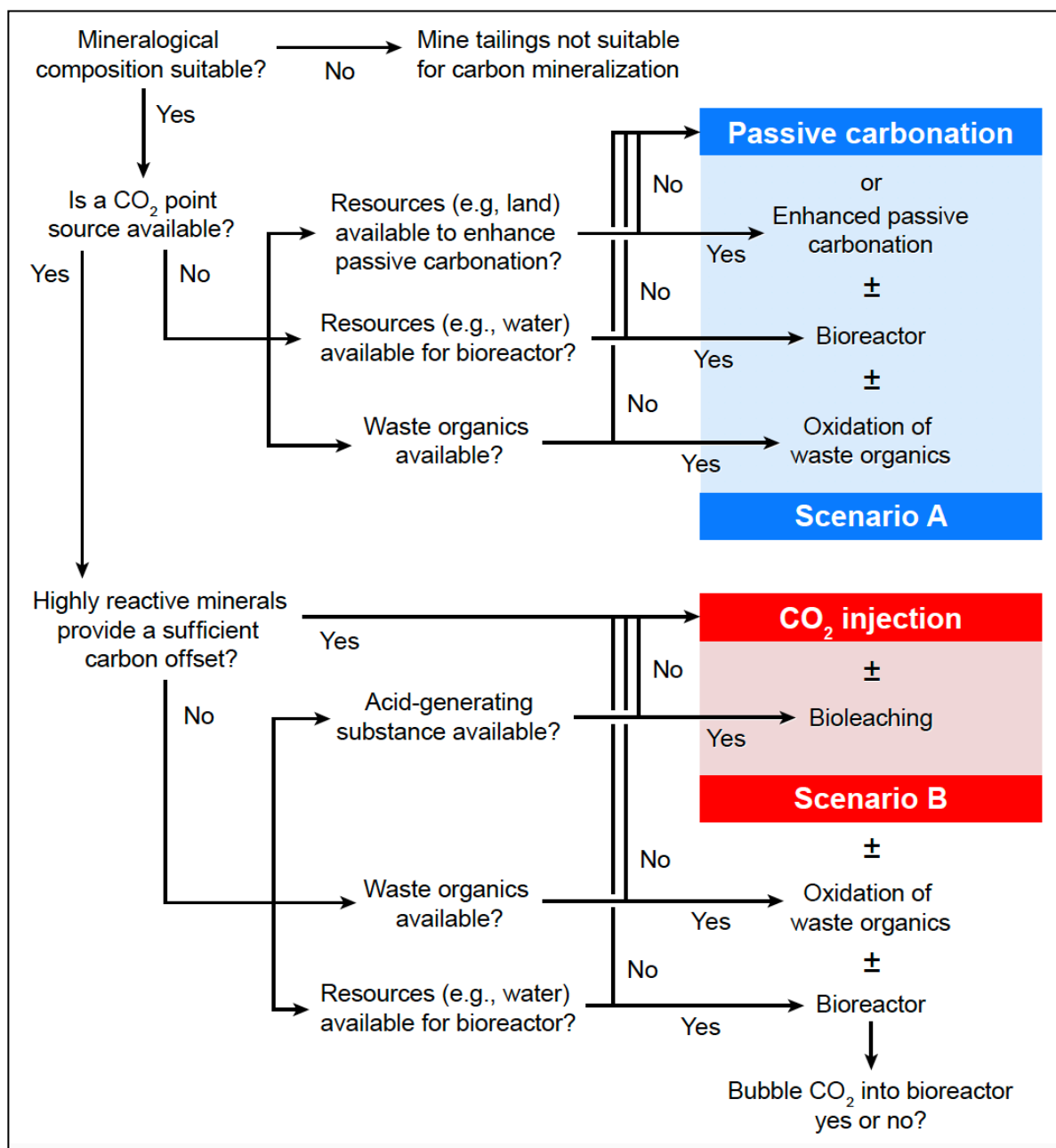
668 can also increase dissolution of minerals and increase the availability of cations for  
669 carbonation (Daval et al., 2013; Power et al., 2014).



670

671 Fig. 5. MIN3P reactive transport modeling of Mount Keith tailings carbonation demonstrating the effect  
672 of tailings deposition rate on brucite carbonation. Reprinted from (Wilson et al., 2014). Copyright  
673 (2014) with permission from Elsevier.

674



675

676 Fig. 6. Decision Tree for selecting mineral carbonation method. In Scenario A, CO<sub>2</sub> is captured from a  
 677 low-concentration stream such as the atmosphere, while in scenario B CO<sub>2</sub> is captured from a high-  
 678 concentration stream such as flue gas (Power et al., 2014). Reproduced from MDPI.

679 Finally, bacteria can be utilized to increase the CO<sub>2</sub> production within tailings.

680 McCutcheon et al. (2017) studied this increase by observing hydromagnesite  
 681 precipitation rates in two 0.5 m<sup>3</sup> passive carbonation cells, one of which was inoculated  
 682 with cyanobacteria. Over a period of 11 weeks, the weight fraction of hydromagnesite  
 683 reached 1.9% for the inoculated sample compared to 1.1% for the bacteria free  
 684 sample, in the top 2-4 cm of the tailings. For inoculated cells the CO<sub>2</sub> uptake reaches

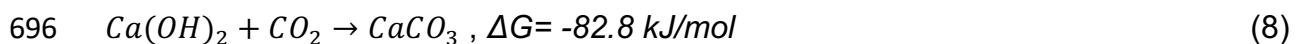
685 137 g cm<sup>-2</sup>, a rate that is much faster when compared to the control experiment in  
686 which CO<sub>2</sub> uptake was estimated to be 27 g cm<sup>-2</sup> (McCutcheon et al., 2016).

## 687 **5. Proposed large-scale passive CCS methods**

688 As shown previously, alkaline wastes can be used as a carbon sink thereby  
689 providing a negative emissions solution. This section summarizes published work in  
690 which methods that can utilize passive carbonation on large scales were proposed,  
691 and it shows some results from their applications.

### 692 **5.1 Direct air capture within designated cells**

693 Abanades et al. (2020) proposed a system, composed of portlandite, that can  
694 capture CO<sub>2</sub> passively over a 6-month time scale, based on equations 8 (Renforth,  
695 2019):



697 The proposed design can sequester 1 x 10<sup>9</sup> kg CO<sub>2</sub> per year by reacting it with  
698 1.68 x 10<sup>9</sup> kg Ca(OH)<sub>2</sub>. It is composed of multiple stacks of 2 x 2 x 0.03 m<sup>3</sup> plates  
699 composed of Ca(OH)<sub>2</sub> having a porosity of 0.5. Based on the reactions kinetics and  
700 air flow considerations, the proposed CCS system occupies a total volume of ~4.6 x  
701 10<sup>7</sup> m<sup>3</sup>, having a total area of ~4.6 x 10<sup>6</sup> m<sup>2</sup> and a height of ~10 m (Abanades et al.,  
702 2020).

703 The proposed design requires a volume that is one to two orders of magnitude  
704 larger than competitive, large-scale direct air capture systems. However, Abanades et  
705 al. (2020) argued that based on cost estimation proposed elsewhere (Guandalini et  
706 al., 2019), their proposed system is feasible. Their cost estimation considers different  
707 factors including the capital cost required for purchasing the oxy-combustion unit  
708 required for CaO production through calcination of CaCO<sub>3</sub>, including fixed, variable

709 and fuel costs. Handling and transportation of structural elements, transporting the  
710 CO<sub>2</sub> produced during calcination to permanent storage as well as land cost were also  
711 incorporated in the cost estimation. They calculated that the cost of capturing 1000 kg  
712 of CO<sub>2</sub> through the proposed design ranges from US\$ 138 - 341, a value that is  
713 significantly lower than the cost of US\$ 600 / 1000 kg CO<sub>2</sub> reported by Climworks  
714 (Tollefson, 2018). At least 67% of this cost is allocated to the capture and storage of  
715 CO<sub>2</sub> produced through oxy-combustion of CaCO<sub>3</sub> which the authors considered to be  
716 the most appropriate source of Ca(OH)<sub>2</sub> that is used in the stacks.

717 McQueen et al. (2020) suggested an alternative process for direct air capture  
718 in which MgO is spread on land to capture CO<sub>2</sub> and form MgCO<sub>3</sub> spontaneously ( $\Delta G$   
719 = -75.9 kJ/mol (Renforth, 2019)). MgO is spread over a large area, and it reacts with  
720 CO<sub>2</sub> to produce MgCO<sub>3</sub>. This process can remove between  $6.0 \times 10^{10}$  and  $1.8 \times 10^{11}$   
721 kgCO<sub>2</sub> y<sup>-1</sup>, requiring an area of  $4 \times 10^8$  -  $1.1 \times 10^9$  m<sup>2</sup>, and it was estimated to cost 48-  
722 159 \$ / 1000 kgCO<sub>2</sub>. The provided cost includes the capital expenditure and operating  
723 expenditure, and the ranges reflect the uncertainties that are associated with the  
724 estimations of different variables, including calcination time and temperature, kiln  
725 efficiency, CO<sub>2</sub> uptake kinetics and capacity, energy prices and other economic  
726 factors. It should be noted that in the methods suggested by Abanades et al. (2020)  
727 and McQueen et al. (2020), CaO and MgO are assumed to be produced through  
728 calcination that produces a CO<sub>2</sub> stream, which is assumed to be stored elsewhere or  
729 sold. Clearly, the efficiency of these methods depends on the availability of points at  
730 which the produced CO<sub>2</sub> is either permanently stored or utilized in different  
731 applications.

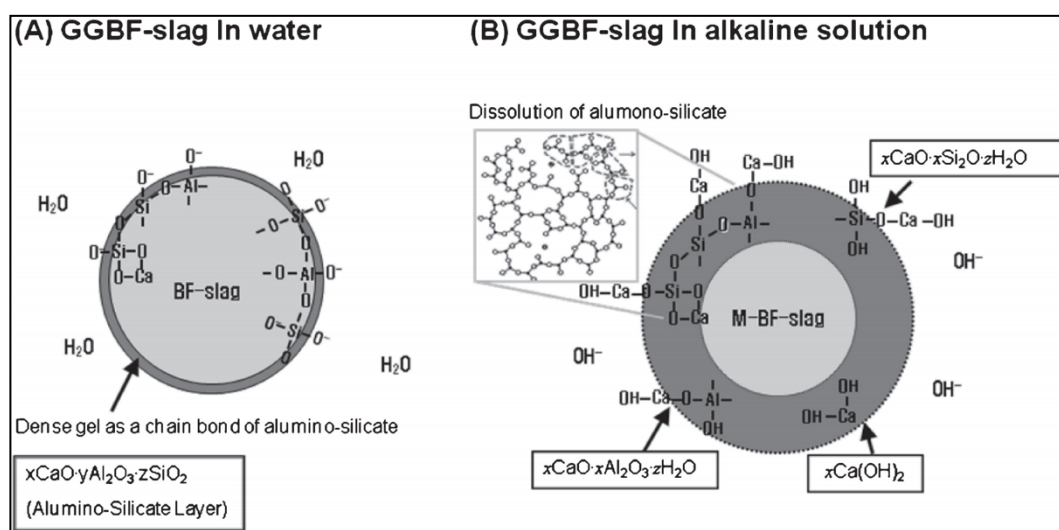
## 732 **5.2 Hot-stage carbonation**

733 Another study proposed carbonation of slag, with flue gas, at an early stage  
734 immediately after the production and disposal of steel slag, in a process referred to as  
735 hot-stage carbonation (Santos et al., 2012). This process is based on enhancing the  
736 carbonation reaction by utilizing the hot temperature of slag to increase the reaction  
737 rate. To test this idea, BOF slag was subjected to calcination in order to remove any  
738  $\text{CaCO}_3$  that might have already formed, and then, using thermogravimetric analysis,  
739 the slag was cooled from 900 °C to 200 °C under  $\text{CO}_2$  flowing at 100 ml/min in two  
740 different experiments: in the first one, the gas composition was 20% vol  $\text{CO}_2$  as such  
741 a stream resembles a typical flue gas from iron and steel industry (Gielen, 2003). In  
742 the second experiment, the gas composition was set to 100%  $\text{CO}_2$ . Pressurization did  
743 not enhance  $\text{CO}_2$  uptake significantly, and Santos et al. (2012) suggested it is more  
744 feasible to use  $\text{CO}_2$  from flue gas for slag carbonation. Slag carbonation seemed to  
745 be diffusion-controlled as the  $\text{CO}_2$  must diffuse through the inert constituent of the slag  
746 to the reactive site from the beginning of the carbonation process (Santos et al., 2012).

## 747 **5.3 Reactivity enhancement by aqueous treatment**

748 Alkaline pretreatment has been proposed to enhance leaching behavior and  
749 carbonation capacity of slag (Chen et al., 2019). The proposed carbonation  
750 enhancement method involves pretreating slag with alkaline solution since, as shown  
751 in a previous study (You et al., 2011) and illustrated in Fig. 7, when slag comes into  
752 contact with water, a dense layer of aluminosilicates may form and inhibit the  
753 carbonation reaction. This layer can be broken down upon the addition of alkaline  
754 sources and then converted to hydrated calcium phases, thereby producing more  
755 phases that can be carbonated to  $\text{CaCO}_3$  (Chen et al., 2019; Matsushita et al., 2000).

756 To confirm this hypothesis, TGA analysis was carried out to determine the  
 757 extent of carbonation for raw slag, and of the one that was pretreated with 1 M NaOH  
 758 at a liquid/solid ratio of 10 mL/g prior to a long term (4-weeks) humidification. By  
 759 measuring the weight loss between 600 and 800 °C, the amount of CaCO<sub>3</sub> can be  
 760 calculated. It was demonstrated that the amount of CO<sub>2</sub> captured within the pretreated  
 761 slag was higher, as demonstrated in the calcite formation which was 17.05 and 50.68  
 762 mg CaCO<sub>3</sub> g<sup>-1</sup> slag, for the raw slag and pretreated slag, respectively.

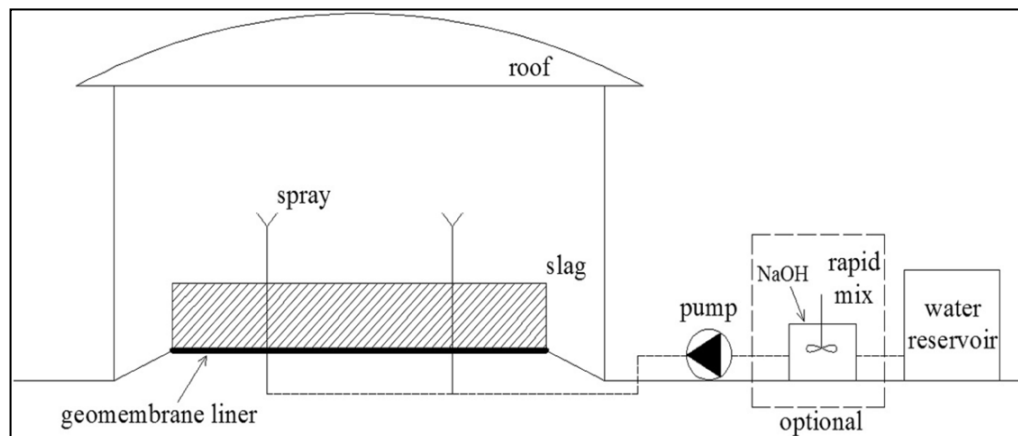


763

764 Fig. 7. Demonstration of aluminosilicate dissolution upon introducing NaOH to ground granulated  
 765 blast furnace (GGBF) slag. Reprinted from You et al. (2011), Copyright (2011) with permission from  
 766 The Japan Institute of Metals and Materials

767 Additionally, a waste management practice was proposed to enhance the  
 768 carbonation, reduce leachate pH and allow for reactivity enhancement of the slag  
 769 (Chen et al., 2019). Portrayed in Fig. 8, the method suggests placing the slag under a  
 770 roof to limit the uncontrolled introduction of water. A geomembrane is also introduced  
 771 to prevent leachate from reaching the surface beneath the slag. Finally, NaOH solution  
 772 can be sprayed over the slag to enhance the carbonation reaction. This method,  
 773 however, depends on the availability and cost of NaOH. Additionally, the emissions  
 774 associated with NaOH manufacturing should also be considered to estimate the net  
 775 CO<sub>2</sub> uptake through this process.





776

777 Fig. 8. Proposed slag carbonation method. Reprinted from (Chen et al., 2019). Copyright (2019) with  
778 permission from Elsevier.

## 779 6. Points for future research

### 780 6.1 Economic valuation of passive carbonation

781 Understanding the economics of CCS projects provides incentives for  
782 enterprises to develop CCS technologies and allow decision-makers to formulate  
783 policies that promote development for CCS technologies (J. Li et al., 2019). As  
784 explained earlier, there are several methods that can enhance mineral carbonation,  
785 and implementing them is associated with the cost related to area requirement, size  
786 reduction and establishing and maintaining piping systems for CO<sub>2</sub> delivery (Song et  
787 al., 2021; Wilson et al., 2014). There is a lack in understanding the economics of  
788 passive mineral carbonation. Valuation of carbon capture projects has been carried  
789 using different methodologies, including optimization models, process simulation and  
790 real options valuation (J. Li et al., 2019). One interesting method is the real options  
791 (RO) valuation (Dixit and Pindyck, 2012), which is considered as a continuation of  
792 financial options theory in that “firms with discretionary investment opportunities have  
793 the right—but are under no obligation—to acquire expected cash flows by making an  
794 investment on or before the date that the (investment) opportunity ceases to exist  
795 (Glantz and Mun, 2011).” RO valuation has been used to study CCS projects,

796 considering several sources of uncertainties, such as policy, carbon prices,  
797 government incentive, and technological changes, as summarized by (H. Li et al.,  
798 2019) and the references therein. Additionally, it has been applied to CCS projects  
799 that involve CO<sub>2</sub> storage in geological formations or through using amine solution to  
800 absorb CO<sub>2</sub> (Ding et al., 2020; J. Li et al., 2019).

801 To our knowledge, only a single study (Power et al., 2014) explained about  
802 using RO to evaluate passive CO<sub>2</sub> mineralization projects. Investment in CCS  
803 technologies should be evaluated through the RO valuation since by doing so, a  
804 company can develop such technologies even when the CO<sub>2</sub> price is low, and it will  
805 have the right, but not the obligation, to apply such technologies when the CO<sub>2</sub> price  
806 becomes more accurate, and CCS becomes economically beneficial (Power et al.,  
807 2014). Passive carbonation is simple compared to other carbon capture technologies,  
808 and as such can have relatively low operation and transportation costs. Research on  
809 techno-economical evaluation can give confidence for mining companies to invest and  
810 apply passive carbonation techniques, and it provides an area of fundamental  
811 research.

## 812 **6.2 Mobility of transition elements**

813 There have been several studies showing that mining wastes can be a vital  
814 source of different transition metals (Gomes et al., 2016). Nevertheless, it has been  
815 argued that carbonation of alkaline wastes may reduce their environmental burdens  
816 (Bobicki et al., 2012; Mayes et al., 2008b; Renforth, 2019). For example, Hamilton et  
817 al. (2018) analyzed the mobility of transition elements during passive weathering and  
818 CO<sub>2</sub> sequestration within the chrysotile deposits at Woodsreef. Upon weathering,  
819 dissolution of serpentine and brucite released these elements, however they were  
820 captured upon precipitation of carbonates, either by substituting the Mg and Fe atoms

821 of the hydromagnesite and pyroaurite, or by being physically trapped within carbonate  
822 cement (Hamilton et al., 2018). As there were no detectable concentrations of  
823 transition metals within the mine pit water, Hamilton et al. (2018) concluded that  
824 mineral carbonation did not release toxic metals. While Hamilton et al. (2018)  
825 demonstrated that carbonates formed during CO<sub>2</sub> mineralization can also sequester  
826 transition metals, they also mentioned other issues that should be highlighted in future  
827 research. For example, hydrated carbonate such as nesquehonite transform to  
828 hydromagnesite and then to magnesite. It is not clear how this transformation affects  
829 the sequestered metals. Additionally, Mayes et al. (2008b) recommended examining  
830 the long-term stability of these metals in different precipitates under different  
831 conditions. Carbonation of other alkaline wastes may have different consequences on  
832 metals leaching. For example, the carbonation of slag was found to have a mixed  
833 effect on metals leaching – it decreased the leaching of barium, nickel and cobalt  
834 though it increased the leaching of chromium and vanadium (Santos et al., 2012). The  
835 carbonation of different alkaline wastes leads to the precipitation of different  
836 carbonates such as calcite, which may interact differently with ecotoxic metals,  
837 presenting an avenue for future research.

### 838 **6.3 Life cycle assessment (LCA) consideration**

839 LCA is a scientific method that evaluates the environmental impact of a process,  
840 quantitatively and qualitatively, throughout its life span (Li et al., 2022). LCA analysis  
841 measures different environmental impacts, such as air pollution, global warming,  
842 ecological toxicity, waste generation and resources depletion associated with a  
843 particular process, to ensure that it can actually solve an environmental problem rather  
844 than shifting it to another problem (Kikuchi, 2016). For example, Butera et al. (2015)  
845 highlighted that when demolition wastes are used in an unbound form, metals may

846 leach out and pollute the environment. Butera et al. (2015) highlighted that when LCA  
847 studies are performed, leaching is not always considered, or the used data may not  
848 reflect actual leaching behavior. Nevertheless, as carbonation of construction and  
849 demolition wastes may lower the leaching of metals, Butera et al. (2015) suggested  
850 that further research should be directed toward this issue to provide better  
851 understanding of environmental impacts associated with the carbonation of demolition  
852 wastes.

853         The physical properties of alkaline wastes may dictate having auxiliary  
854 operations such as crushing and transportation (Collins, 2010). Such steps may cause  
855 mineral carbonation to be less effective compared to geological sequestration and to  
856 cause other environmental problems (Giannoulakis et al., 2014). To our knowledge,  
857 however, there are limited LCA studies that evaluate the environmental impact of  
858 waste management practices that can enhance passive carbonation. For example,  
859 using flue gas to carbonate slag requires less transportation since both materials are  
860 produced in close locations, but may result in other emissions that are associated with  
861 maintaining and operating a CO<sub>2</sub> piping system as well as slag pulverization. LCA can  
862 assist in understanding the overall CO<sub>2</sub> uptake through this carbonation route and  
863 comparing it to other methods. Unlike mine waste, slag is produced at a larger size,  
864 and it must be pulverized before carbonation can take place. This makes mining  
865 wastes “low hanging fruits” as described by Kelemen et al. (2020), since they are  
866 already produced with large surface area as a consequence of mineral processing.

867         Finally, it should be noted that current LCA models require the calculation of  
868 the amount of industrial wastes that must be treated to capture a given amount of CO<sub>2</sub>.  
869 This information can be calculated from the reaction rate laws that are available in the  
870 literature (e.g., Chang et al. (2013); Thom et al. (2013)). However, some interactions

871 between the operating conditions can result in unexpected CO<sub>2</sub> uptake. For example,  
872 Poletini et al. (2016b) demonstrated that under 1 bar 50 °C and 40% CO<sub>2</sub>, steel slag  
873 can capture CO<sub>2</sub> at an amount of 30 g CO<sub>2</sub>/100g slag compared to 33 g CO<sub>2</sub>/100 g  
874 slag captured under more elevated conditions of 10 bar, 100% CO<sub>2</sub> and 100 °C. This  
875 indicates that there is room for further kinetic analysis of carbonation since the  
876 reduction of operating conditions and CO<sub>2</sub> concentration reduces the environmental  
877 impact of the mineral carbonation process.

## 878 **7. Concluding remarks**

879 There is growing evidence indicating that passive carbonation of alkaline  
880 wastes occurs to an extent that can reduce or offset the amount of CO<sub>2</sub> emitted from  
881 energy-intensive industries, such as steelmaking and mining. Globally, alkaline wastes  
882 are produced at a rate of  $7 \times 10^{12}$  -  $1.7 \times 10^{13}$  kg y<sup>-1</sup> and by 2100, they are estimated  
883 to have an annual CO<sub>2</sub> capture potential of  $2.9 \times 10^{12}$  to  $8.5 \times 10^{12}$  kg y<sup>-1</sup> (Renforth,  
884 2019). However, studies show that the CO<sub>2</sub> uptake potential of alkaline wastes is  
885 underutilized due to several factors such as slow dissolution kinetics of silicate  
886 minerals, low CO<sub>2</sub> ingress into alkaline wastes and due to the passivation of reactive  
887 surfaces as a result of silica gel polymerization and carbonates precipitation. These  
888 challenges can be overcome through the application of different waste management  
889 practices such as controlling waste deposition rate, controlling the water saturation  
890 and the watering frequency and enhancing the contact between these wastes and the  
891 atmosphere. While the reviewed literature demonstrates that these methods can result  
892 in larger CO<sub>2</sub> uptake, the proposed methods should be evaluated through lifecycle  
893 assessment, which in turn requires adequate knowledge of leaching mechanisms of  
894 different ecotoxic metals that reside in the alkaline wastes. Although the proposed  
895 waste management practices are simple, they are associated with different costs

896 related to the area footprint and maintenance of CO<sub>2</sub> piping systems. Consequently,  
897 they should be evaluated from a techno-economic perspective.

## 898 **Acknowledgement**

899 Faisal W. K. Khudhur acknowledges generous support from the University of Glasgow  
900 Lord Kelvin/Adam Smith Ph.D. scholarship. Three anonymous reviewers are  
901 acknowledged for their comments that significantly enhanced this manuscript.

## 902 **8. References**

- 903
- 904 Abanades, J.C., Criado, Y.A., Fernández, J.R., 2020. An air CO<sub>2</sub> capture system based on the  
905 passive carbonation of large Ca(OH)<sub>2</sub> structures. *Sustain. Energy Fuels* 4, 3409–3417.  
906 <https://doi.org/10.1039/D0SE00094A>
- 907 Alcoa, 2012. Long Term Residue Management Strategy Kwinana 2012 [WWW Document].  
908 URL  
909 [https://www.alcoa.com/australia/en/pdf/kwinana\\_refinery\\_itrms\\_report\\_2012.pdf](https://www.alcoa.com/australia/en/pdf/kwinana_refinery_itrms_report_2012.pdf)  
910 (accessed 12.25.21).
- 911 Amiotte Suchet, P., Probst, J.-L., Ludwig, W., 2003. Worldwide distribution of continental  
912 rock lithology: Implications for the atmospheric/soil CO<sub>2</sub> uptake by continental  
913 weathering and alkalinity river transport to the oceans. *Global Biogeochem. Cycles* 17.  
914 <https://doi.org/10.1029/2002GB001891>
- 915 Archer, D., 2007. *Global Warming: Understanding the Forecast*, 1st ed. Blackwell Publishing.
- 916 Assima, G.P., Larachi, F., Beaudoin, G., Molson, J., 2013. Dynamics of carbon dioxide uptake  
917 in chrysotile mining residues – Effect of mineralogy and liquid saturation. *Int. J. Greenh.*  
918 *Gas Control* 12, 124–135. <https://doi.org/10.1016/J.IJGGC.2012.10.001>
- 919 Assima, G.P., Larachi, F., Beaudoin, G., Molson, J., 2012. CO<sub>2</sub> Sequestration in Chrysotile  
920 Mining Residues—Implication of Watering and Passivation under Environmental  
921 Conditions. *Ind. Eng. Chem. Res.* 51, 8726–8734. <https://doi.org/10.1021/IE202693Q>
- 922 Assima, G.P., Larachi, F., Molson, J., Beaudoin, G., 2014a. Impact of temperature and oxygen  
923 availability on the dynamics of ambient CO<sub>2</sub> mineral sequestration by nickel mining  
924 residues. *Chem. Eng. J.* 240, 394–403. <https://doi.org/10.1016/J.CEJ.2013.12.010>
- 925 Assima, G.P., Larachi, F., Molson, J., Beaudoin, G., 2014b. New tools for stimulating  
926 dissolution and carbonation of ultramafic mining residues. *Can. J. Chem. Eng.* 92, 2029–  
927 2038. <https://doi.org/10.1002/CJCE.22066>
- 928 Azdarpour, A., Asadullah, M., Mohammadian, E., Hamidi, H., Junin, R., Karaei, M.A., 2015. A  
929 review on carbon dioxide mineral carbonation through pH-swing process. *Chem. Eng. J.*  
930 279, 615–630. <https://doi.org/10.1016/J.CEJ.2015.05.064>
- 931 Baker, D.R., Mancini, L., Polacci, M., Higgins, M.D., Gualda, G.A.R., Hill, R.J., Rivers, M.L.,  
932 2012. An introduction to the application of X-ray microtomography to the three-  
933 dimensional study of igneous rocks. *Lithos* 148, 262–276.  
934 <https://doi.org/10.1016/j.lithos.2012.06.008>
- 935 Bea, S.A., Wilson, S.A., Mayer, K.U., Dipple, G.M., Power, I.M., Gamazo, P., 2012. Reactive

- 936 Transport Modeling of Natural Carbon Sequestration in Ultramafic Mine Tailings.  
937 Vadose Zo. J. 11, vzj2011.0053. <https://doi.org/10.2136/vzj2011.0053>
- 938 Beinlich, A., Austrheim, H., 2012. In situ sequestration of atmospheric CO<sub>2</sub> at low  
939 temperature and surface cracking of serpentinized peridotite in mine shafts. *Chem.*  
940 *Geol.* 332–333, 32–44. <https://doi.org/10.1016/j.chemgeo.2012.09.015>
- 941 Bobicki, E.R., Liu, Q., Xu, Z., Zeng, H., 2012. Carbon capture and storage using alkaline  
942 industrial wastes. *Prog. Energy Combust. Sci.* 38, 302–320.  
943 <https://doi.org/10.1016/j.pecs.2011.11.002>
- 944 Bodor, M., Santos, R.M., Kriskova, L., Elsen, J., Vlad, M., Van Gerven, T., 2013. Susceptibility  
945 of mineral phases of steel slags towards carbonation: mineralogical, morphological and  
946 chemical assessment. *Eur. J. Mineral.* 533–549. [https://doi.org/10.1127/0935-](https://doi.org/10.1127/0935-1221/2013/0025-2300)  
947 [1221/2013/0025-2300](https://doi.org/10.1127/0935-1221/2013/0025-2300)
- 948 Boone, M.A., Nielsen, P., De Kock, T., Boone, M.N., Quaghebeur, M., Cnudde, V., 2014.  
949 Monitoring of Stainless-Steel Slag Carbonation Using X-ray Computed  
950 Microtomography. *Environ. Sci. Technol.* 48, 674–680.  
951 <https://doi.org/10.1021/es402767q>
- 952 Brown, R., Brownlow, J., Krynen, J., 1992. Manilla - Narrabri 1:250000 Metallogenic Map,  
953 SH/56-9, SH/55-12: Metallogenic Study and Mineral Deposit Data Sheets. *NSW Geol.*  
954 *Surv., Metallogenic Map. Ser.*
- 955 Brown, T.J., Idoine, N.E., Wrighton, E.R., Raycraft, E.R., Hobbs, S.F., Shaw, R.A., Everett, P.,  
956 Kresse, C., Deady, E.A., Bide, T., 2020. World Mineral Production 2014-2018 [WWW  
957 Document]. *Br. Geol. Surv.* URL  
958 <https://www2.bgs.ac.uk/mineralsUK/statistics/worldStatistics.html>
- 959 Buis, A., 2019. The Atmosphere: Getting a Handle on Carbon Dioxide – Climate Change: Vital  
960 Signs of the Planet [WWW Document]. URL [https://climate.nasa.gov/news/2915/the-](https://climate.nasa.gov/news/2915/the-atmosphere-getting-a-handle-on-carbon-dioxide/)  
961 [atmosphere-getting-a-handle-on-carbon-dioxide/](https://climate.nasa.gov/news/2915/the-atmosphere-getting-a-handle-on-carbon-dioxide/) (accessed 1.18.22).
- 962 Bullock, L.A., Yang, A., Darton, R.C., 2022. Kinetics-informed global assessment of mine  
963 tailings for CO<sub>2</sub> removal. *Sci. Total Environ.* 808, 152111.  
964 <https://doi.org/10.1016/J.SCITOTENV.2021.152111>
- 965 Butera, S., Christensen, T.H., Astrup, T.F., 2015. Life cycle assessment of construction and  
966 demolition waste management. *Waste Manag.* 44, 196–205.  
967 <https://doi.org/10.1016/J.WASMAN.2015.07.011>
- 968 Chang, E.E., Chiu, A.C., Pan, S.Y., Chen, Y.H., Tan, C.S., Chiang, P.C., 2013. Carbonation of  
969 basic oxygen furnace slag with metalworking wastewater in a slurry reactor. *Int. J.*  
970 *Greenh. Gas Control* 12, 382–389. <https://doi.org/10.1016/j.ijggc.2012.11.026>
- 971 Chang, E.E., Pan, S.Y., Chen, Y.H., Tan, C.S., Chiang, P.C., 2012. Accelerated carbonation of  
972 steelmaking slags in a high-gravity rotating packed bed. *J. Hazard. Mater.* 227–228, 97–  
973 106. <https://doi.org/10.1016/j.jhazmat.2012.05.021>
- 974 Chen, B., Yoon, S., Zhang, Y., Han, L., Choi, Y., 2019. Reduction of steel slag leachate pH via  
975 humidification using water and aqueous reagents. *Sci. Total Environ.* 671, 598–607.  
976 <https://doi.org/10.1016/j.scitotenv.2019.03.362>
- 977 Chiang, P.C., Pan, S.Y., 2017. Carbon dioxide mineralization and utilization, Carbon Dioxide  
978 Mineralization and Utilization. <https://doi.org/10.1007/978-981-10-3268-4>
- 979 Chukwuma, J.S., Pullin, H., Renforth, P., 2021. Assessing the carbon capture capacity of  
980 South Wales' legacy iron and steel slag. *Miner. Eng.* 173, 107232.  
981 <https://doi.org/10.1016/J.MINENG.2021.107232>
- 982 Collins, F., 2010. Inclusion of carbonation during the life cycle of built and recycled concrete:

- 983 Influence on their carbon footprint. *Int. J. Life Cycle Assess.* 15, 549–556.  
984 <https://doi.org/10.1007/S11367-010-0191-4/TABLES/5>
- 985 Daval, D., 2018. Carbon dioxide sequestration through silicate degradation and carbon  
986 mineralisation: promises and uncertainties. *npj Mater. Degrad.* 2, 1–4.  
987 <https://doi.org/10.1038/s41529-018-0035-4>
- 988 Daval, D., Hellmann, R., Martinez, I., Gangloff, S., Guyot, F., 2013. Lizardite serpentine  
989 dissolution kinetics as a function of pH and temperature, including effects of elevated  
990 pCO<sub>2</sub>. *Chem. Geol.* 351, 245–256. <https://doi.org/10.1016/j.chemgeo.2013.05.020>
- 991 Daval, D., Martinez, I., Corvisier, J., Findling, N., Goffé, B., Guyot, F., 2009. Carbonation of  
992 Ca-bearing silicates, the case of wollastonite: Experimental investigations and kinetic  
993 modeling. *Chem. Geol.* 265, 63–78. <https://doi.org/10.1016/J.CHEMGEO.2009.01.022>
- 994 Dembicki, Jr., H., 2017. Source Rock Evaluation, in: *Practical Petroleum Geochemistry for*  
995 *Exploration and Production*. Elsevier, pp. 61–133. [https://doi.org/10.1016/B978-0-12-](https://doi.org/10.1016/B978-0-12-803350-0.00003-9)  
996 [803350-0.00003-9](https://doi.org/10.1016/B978-0-12-803350-0.00003-9)
- 997 Ding, H., Zheng, H., Liang, X., Ren, L., 2020. Getting ready for carbon capture and storage in  
998 the iron and steel sector in China: Assessing the value of capture readiness. *J. Clean.*  
999 *Prod.* 244, 118953. <https://doi.org/10.1016/j.jclepro.2019.118953>
- 1000 Dixit, A.K., Pindyck, R.S., 2012. *Investment Under Uncertainty*. Princeton University Press.
- 1001 Dlugogorski, B.Z., Balucan, R.D., 2014. Dehydroxylation of serpentine minerals: Implications  
1002 for mineral carbonation. *Renew. Sustain. Energy Rev.* 31, 353–367.  
1003 <https://doi.org/10.1016/J.RSER.2013.11.002>
- 1004 Edwards, K.J., Goebel, B.M., 1999. Geomicrobiology of Pyrite (FeS<sub>2</sub>) Dissolution: Case Study  
1005 at Iron Mountain, California. *Geomicrobiol. J.* 16, 155–179.  
1006 <https://doi.org/10.1080/014904599270668>
- 1007 Engström, F., Adolfsen, D., Samuelsson, C., Sandström, Å., Björkman, B., 2013. A study of  
1008 the solubility of pure slag minerals. *Miner. Eng.* 41, 46–52.  
1009 <https://doi.org/10.1016/J.MINENG.2012.10.004>
- 1010 Gaillardet, J., Dupré, B., Louvat, P., Allègre, C.J., 1999. Global silicate weathering and CO<sub>2</sub>  
1011 consumption rates deduced from the chemistry of large rivers. *Chem. Geol.* 159, 3–30.  
1012 [https://doi.org/10.1016/S0009-2541\(99\)00031-5](https://doi.org/10.1016/S0009-2541(99)00031-5)
- 1013 Gao, X., Jiang, L., Mao, Y., Yao, B., Jiang, P., 2021. Progress, Challenges, and Perspectives of  
1014 Bioleaching for Recovering Heavy Metals from Mine Tailings. *Adsorpt. Sci. Technol.*  
1015 2021. <https://doi.org/10.1155/2021/9941979>
- 1016 Gencel, O., Karadag, O., Oren, O.H., Bilir, T., 2021. Steel slag and its applications in cement  
1017 and concrete technology: A review. *Constr. Build. Mater.* 283, 122783.  
1018 <https://doi.org/10.1016/j.conbuildmat.2021.122783>
- 1019 Geoscience Australia, 2018. Aluminium [WWW Document]. URL  
1020 [https://www.ga.gov.au/education/classroom-resources/minerals-energy/australian-](https://www.ga.gov.au/education/classroom-resources/minerals-energy/australian-mineral-facts/aluminium)  
1021 [mineral-facts/aluminium](https://www.ga.gov.au/education/classroom-resources/minerals-energy/australian-mineral-facts/aluminium) (accessed 10.11.20).
- 1022 Giannoulakis, S., Volkart, K., Bauer, C., 2014. Life cycle and cost assessment of mineral  
1023 carbonation for carbon capture and storage in European power generation. *Int. J.*  
1024 *Greenh. Gas Control* 21, 140–157. <https://doi.org/10.1016/j.ijggc.2013.12.002>
- 1025 Gielen, D., 2003. CO<sub>2</sub> removal in the iron and steel industry. *Energy Convers. Manag.* 44,  
1026 1027–1037. [https://doi.org/10.1016/S0196-8904\(02\)00111-5](https://doi.org/10.1016/S0196-8904(02)00111-5)
- 1027 Glantz, M., Mun, J., 2011. Introduction, in: *Credit Engineering for Bankers*. Elsevier, pp. xvii–  
1028 xxi. <https://doi.org/10.1016/B978-0-12-378585-5.10027-2>
- 1029 Goetz, E.R., Riefler, R.G., 2015. Geochemistry of CO<sub>2</sub> in Steel Slag Leach Beds. *Mine Water*



- 1030 Environ. 34, 42–49. <https://doi.org/10.1007/s10230-014-0290-8>
- 1031 Gomes, H.I., Mayes, W.M., Rogerson, M., Stewart, D.I., Burked, I.T., 2016. Alkaline residues  
1032 and the environment: A review of impacts, management practices and opportunities. J.  
1033 Clean. Prod. <https://doi.org/10.1016/j.jclepro.2015.09.111>
- 1034 Gore, M., 2015. Geotechnical Characterization of Bauxite Residue. The University of Texas at  
1035 Austin.
- 1036 Gras, A., Beaudoin, G., Molson, J., Plante, B., 2020. Atmospheric carbon sequestration in  
1037 ultramafic mining residues and impacts on leachate water chemistry at the Dumont  
1038 Nickel Project, Quebec, Canada. Chem. Geol. 546, 119661.  
1039 <https://doi.org/10.1016/j.chemgeo.2020.119661>
- 1040 Gras, A., Beaudoin, G., Molson, J., Plante, B., Bussière, B., Lemieux, J.M., Dupont, P.P., 2017.  
1041 Isotopic evidence of passive mineral carbonation in mine wastes from the Dumont  
1042 Nickel Project (Abitibi, Quebec). Int. J. Greenh. Gas Control 60, 10–23.  
1043 <https://doi.org/10.1016/j.ijggc.2017.03.002>
- 1044 Gras, A., Beaudoin, G., Molson, J., Plante, B., Bussière, B., Lemieux, J.M., Kandji, B., 2015.  
1045 Carbon isotope evidence for passive mineral carbonation of mine wastes from the  
1046 Dumont Nickel Project (Abitibi, Quebec) - ACEME 2015, in: 5th International  
1047 Conference on Accelerated Carbonation for Environmental and Material Engineering.  
1048 New York, USA.
- 1049 Grénman, H., Ramirez, F., Eränen, K., Wärnå, J., Salmi, T., Murzin, D.Y., 2008. Dissolution of  
1050 Mineral Fiber in a Formic Acid Solution: Kinetics, Modeling, and Gelation of the  
1051 Resulting Sol. Ind. Eng. Chem. Res. 47, 9834–9841. <https://doi.org/10.1021/IE800267A>
- 1052 Guandalini, G., Romano, M.C., Ho, M., Wiley, D., Rubin, E.S., Abanades, J.C., 2019. A  
1053 sequential approach for the economic evaluation of new CO<sub>2</sub> capture technologies for  
1054 power plants. Int. J. Greenh. Gas Control 84, 219–231.  
1055 <https://doi.org/10.1016/j.ijggc.2019.03.006>
- 1056 Gunning, P.J., Hills, C.D., Carey, P.J., 2010. Accelerated carbonation treatment of industrial  
1057 wastes. Waste Manag. 30, 1081–1090. <https://doi.org/10.1016/j.wasman.2010.01.005>
- 1058 Hamilton, J.L., Wilson, S.A., Morgan, B., Turvey, C.C., Paterson, D.J., Jowitt, S.M.,  
1059 McCutcheon, J., Southam, G., 2018. Fate of transition metals during passive  
1060 carbonation of ultramafic mine tailings via air capture with potential for metal resource  
1061 recovery. Int. J. Greenh. Gas Control 71, 155–167.  
1062 <https://doi.org/10.1016/j.ijggc.2018.02.008>
- 1063 Hamilton, J.L., Wilson, S.A., Turvey, C.C., Tait, A.W., McCutcheon, J., Fallon, S.J., Southam, G.,  
1064 (In prep). Field-based deployment of an automated geochemical treatment system for  
1065 accelerating carbonation of ultramafic mine tailings: Lessons for pilot projects and  
1066 carbon accounting in mined landscapes. In Preparation.
- 1067 Han, Y.-S., Ji, S., Lee, P.-K., Oh, C., 2017. Bauxite residue neutralization with simultaneous  
1068 mineral carbonation using atmospheric CO<sub>2</sub>. J. Hazard. Mater. 326, 87–93.  
1069 <https://doi.org/10.1016/j.jhazmat.2016.12.020>
- 1070 Harnisch, J., Wing, I.S., Jacoby, H.D., Prinn, R.G., 1998. Primary Aluminum Production:  
1071 Climate Policy, Emissions and Costs. Joint Program Report Series 44.
- 1072 Harrison, A.L., Power, I.M., Dipple, G.M., 2013. Strategies for enhancing carbon  
1073 sequestration in Mg-rich mine tailings, in: Wolkersdorfer, Brown, Figueroa (Eds.),  
1074 IMWA: Reliable Mine Water Technology. IMWA, Golden Colorado, USA.
- 1075 Harrison, A.L., Power, I.M., Dipple, G.M., 2012. Accelerated Carbonation of Brucite in Mine  
1076 Tailings for Carbon Sequestration. Environ. Sci. Technol. 47, 126–134.

- 1077 <https://doi.org/10.1021/ES3012854>
- 1078 Hu, R., Xie, J., Wu, S., Yang, C., Yang, D., 2020. Study of toxicity assessment of heavy metals  
1079 from steel slag and its asphalt mixture. *Materials (Basel)*. 13, 2768.  
1080 <https://doi.org/10.3390/ma13122768>
- 1081 Huh, Y., 2003. Chemical weathering and climate — a global experiment: A review. *Geosci. J.*  
1082 7, 277–288. <https://doi.org/10.1007/BF02910294>
- 1083 Huijgen, W.J.J., Comans, R.N.J., 2005. Carbon dioxide sequestration by mineral carbonation:  
1084 Literature review update 2003-2004.
- 1085 Huijgen, W.J.J., Witkamp, G.J., Comans, R.N.J., 2005. Mineral CO<sub>2</sub> sequestration by steel slag  
1086 carbonation. *Environ. Sci. Technol.* 39, 9676–9682. <https://doi.org/10.1021/es050795f>
- 1087 Indian and Northern Affairs Canada, 2008. The Big Picture Yukon's Large Contaminated Sites  
1088 [WWW Document]. URL [https://www.aadnc-aandc.gc.ca/DAM/DAM-INTER-](https://www.aadnc-aandc.gc.ca/DAM/DAM-INTER-YT/STAGING/texte-text/pubs-tbp-pdf_1316463525304_eng.pdf)  
1089 [YT/STAGING/texte-text/pubs-tbp-pdf\\_1316463525304\\_eng.pdf](https://www.aadnc-aandc.gc.ca/DAM/DAM-INTER-YT/STAGING/texte-text/pubs-tbp-pdf_1316463525304_eng.pdf) (accessed 3.11.21).
- 1090 IPCC, 2021. Summary for Policymakers. In: *Climate Change 2021: The Physical Science Basis.*  
1091 Contribution of Working Group I to the Sixth Assessment Report of the  
1092 Intergovernmental Panel on Climate Change.
- 1093 Jorat, M.E., Goddard, M.A., Manning, P., Lau, H.K., Ngeow, S., Sohi, S.P., Manning, D.A.C.,  
1094 2020. Passive CO<sub>2</sub> removal in urban soils: Evidence from brownfield sites. *Sci. Total*  
1095 *Environ.* 703, 135573. <https://doi.org/10.1016/j.scitotenv.2019.135573>
- 1096 Kandji, E.H.B., Plante, B., Bussière, B., Beaudoin, G., Dupont, P.P., 2017. Kinetic testing to  
1097 evaluate the mineral carbonation and metal leaching potential of ultramafic tailings:  
1098 Case study of the Dumont Nickel Project, Amos, Québec. *Appl. Geochemistry* 84, 262–  
1099 276. <https://doi.org/10.1016/j.apgeochem.2017.07.005>
- 1100 Kelemen, P.B., Matter, J., Streit, E.E., Rudge, J.F., Curry, W.B., Blusztajn, J., 2011. Rates and  
1101 mechanisms of mineral carbonation in peridotite: Natural processes and recipes for  
1102 enhanced, in situ CO<sub>2</sub> capture and storage. *Annu. Rev. Earth Planet. Sci.* 39, 545–576.  
1103 <https://doi.org/10.1146/annurev-earth-092010-152509>
- 1104 Kelemen, P.B., McQueen, N., Wilcox, J., Renforth, P., Dipple, G., Vankeuren, A.P., 2020.  
1105 Engineered carbon mineralization in ultramafic rocks for CO<sub>2</sub> removal from air: Review  
1106 and new insights. *Chem. Geol.* 550, 119628.  
1107 <https://doi.org/10.1016/j.chemgeo.2020.119628>
- 1108 Khaitan, S., Dzombak, D.A., Swallow, P., Schmidt, K., Fu, J., Lowry, G. V., 2010. Field  
1109 Evaluation of Bauxite Residue Neutralization by Carbon Dioxide, Vegetation, and  
1110 Organic Amendments. *J. Environ. Eng.* 136, 1045–1053.  
1111 [https://doi.org/10.1061/\(ASCE\)EE.1943-7870.0000230](https://doi.org/10.1061/(ASCE)EE.1943-7870.0000230)
- 1112 Kikuchi, Y., 2016. Life Cycle Assessment, in: *Plant Factory: An Indoor Vertical Farming System*  
1113 *for Efficient Quality Food Production.* Academic Press, pp. 321–329.  
1114 <https://doi.org/10.1016/B978-0-12-801775-3.00024-X>
- 1115 Kriskova, L., Pontikes, Y., Pandelaers, L., Cizer, Ö., Jones, P.T., Van Balen, K., Blanpain, B.,  
1116 2013. Effect of High Cooling Rates on the Mineralogy and Hydraulic Properties of  
1117 Stainless Steel Slags. *Metall. Mater. Trans. B* 2013 44, 1173–1184.  
1118 <https://doi.org/10.1007/S11663-013-9894-9>
- 1119 Lai, J.L., Shek, C.H., Ho Lo, K., 2012. *Stainless Steel An Introduction and Their Recent*  
1120 *Developments : An Introduction and Their Recent Developments.* Bentham Science  
1121 Publishers, ProQuest Ebook Central,  
1122 <https://ebookcentral.proquest.com/lib/gla/detail.action?docID=877022>.
- 1123 Lechat, K., Lemieux, J.M., Molson, J., Beaudoin, G., Hébert, R., 2016. Field evidence of CO<sub>2</sub>

- 1124 sequestration by mineral carbonation in ultramafic milling wastes, Thetford Mines,  
1125 Canada. *Int. J. Greenh. Gas Control* 47, 110–121.  
1126 <https://doi.org/10.1016/j.ijggc.2016.01.036>
- 1127 LECO Corporation, 2008. SC-144DR Sulfur/Carbon Determinator Specification Sheet.  
1128 Li, H., Jiang, H.D., Yang, B., Liao, H., 2019. An analysis of research hotspots and modeling  
1129 techniques on carbon capture and storage. *Sci. Total Environ.* 687, 687–701.  
1130 <https://doi.org/10.1016/j.scitotenv.2019.06.013>
- 1131 Li, J., Hou, Y., Wang, P., Yang, B., 2019. A Review of carbon capture and storage project  
1132 investment and operational decision-making based on bibliometrics. *Energies* 12.  
1133 <https://doi.org/10.3390/en12010023>
- 1134 Li, L., Ling, T.-C., Pan, S.-Y., 2022. Environmental benefit assessment of steel slag utilization  
1135 and carbonation: A systematic review. *Sci. Total Environ.* 806, 150280.  
1136 <https://doi.org/10.1016/j.scitotenv.2021.150280>
- 1137 Liu, W., Teng, L., Rohani, S., Qin, Z., Zhao, B., Xu, C.C., Ren, S., Liu, Q., Liang, B., 2021. CO<sub>2</sub>  
1138 mineral carbonation using industrial solid wastes: A review of recent developments.  
1139 *Chem. Eng. J.* 416, 129093. <https://doi.org/10.1016/J.CEJ.2021.129093>
- 1140 Marinković, S.B., Malešev, M., Ignjatović, I., 2014. Life cycle assessment (LCA) of concrete  
1141 made using recycled concrete or natural aggregates. *Eco-Efficient Constr. Build. Mater.*  
1142 *Life Cycle Assess. (LCA), Eco-Labeling Case Stud.* 239–266.  
1143 <https://doi.org/10.1533/9780857097729.2.239>
- 1144 Matsushita, F., Aono, Y., Shibata, S., 2000. Carbonation degree of autoclaved aerated  
1145 concrete. *Cem. Concr. Res.* 30, 1741–1745. [https://doi.org/10.1016/S0008-8846\(00\)00424-5](https://doi.org/10.1016/S0008-8846(00)00424-5)
- 1147 Mayes, W.M., Gozzard, E., Potter, H.A.B., Jarvis, A.P., 2008a. Quantifying the importance of  
1148 diffuse minewater pollution in a historically heavily coal mined catchment. *Environ.*  
1149 *Pollut.* 151, 165–175. <https://doi.org/10.1016/j.envpol.2007.02.008>
- 1150 Mayes, W.M., Jarvis, A.P., Burke, I.T., Walton, M., Feigl, V., Klebercz, O., Gruiz, K., 2011.  
1151 Dispersal and Attenuation of Trace Contaminants Downstream of the Ajka Bauxite  
1152 Residue (Red Mud) Depository Failure, Hungary. *Environ. Sci. Technol.* 45, 5147–5155.  
1153 <https://doi.org/10.1021/es200850y>
- 1154 Mayes, W.M., Riley, A.L., Gomes, H.I., Brabham, P., Hamlyn, J., Pullin, H., Renforth, P., 2018.  
1155 Atmospheric CO<sub>2</sub> Sequestration in Iron and Steel Slag: Consett, County Durham,  
1156 United Kingdom. *Environ. Sci. Technol.* 52, 7892–7900.  
1157 <https://doi.org/10.1021/acs.est.8b01883>
- 1158 Mayes, W.M., Younger, P. L., Aumônier, J., 2006. Buffering of Alkaline Steel Slag Leachate  
1159 across a Natural Wetland. *Environ. Sci. Technol.* 40, 1237–1243.  
1160 <https://doi.org/10.1021/ES051304U>
- 1161 Mayes, W.M., Younger, P.L., Aumônier, J., 2008b. Hydrogeochemistry of alkaline steel slag  
1162 leachates in the UK. *Water. Air. Soil Pollut.* 195, 35–50.  
1163 <https://doi.org/10.1007/S11270-008-9725-9/TABLES/4>
- 1164 McCutcheon, J., Turvey, C.C., Wilson, S.A., Hamilton, J.L., Southam, G., 2017. Experimental  
1165 deployment of microbial mineral carbonation at an asbestos mine: Potential  
1166 applications to carbon storage and tailings stabilization. *Minerals* 7, 15–18.  
1167 <https://doi.org/10.3390/min7100191>
- 1168 McCutcheon, J., Wilson, S.A., Southam, G., 2016. Microbially Accelerated Carbonate Mineral  
1169 Precipitation as a Strategy for in Situ Carbon Sequestration and Rehabilitation of  
1170 Asbestos Mine Sites. *Environ. Sci. Technol.* 50, 1419–1427.

- 1171 <https://doi.org/10.1021/ACS.EST.5B04293>
- 1172 McQueen, N., Kelemen, P., Dipple, G., Renforth, P., Wilcox, J., 2020. Ambient weathering of  
1173 magnesium oxide for CO<sub>2</sub> removal from air. *Nat. Commun.* 2020 11 11, 1–10.  
1174 <https://doi.org/10.1038/s41467-020-16510-3>
- 1175 Mervine, E.M., Wilson, S.A., Power, I.M., Dipple, G.M., Turvey, C.C., Hamilton, J.L.,  
1176 Vanderzee, S., Raudsepp, M., Southam, C., Matter, J.M., Kelemen, P.B., Stiefenhofer, J.,  
1177 Miya, Z., Southam, G., 2018. Potential for offsetting diamond mine carbon emissions  
1178 through mineral carbonation of processed kimberlite: an assessment of De Beers mine  
1179 sites in South Africa and Canada. *Mineral. Petrol.* 112, 755–765.  
1180 <https://doi.org/10.1007/s00710-018-0589-4>
- 1181 Meyer, D.R., 1980. Nutritional problems associated with the establishment of vegetation on  
1182 tailings from an asbestos mine. *Environ. Pollut. Ser. A, Ecol. Biol.* 23, 287–298.  
1183 [https://doi.org/10.1016/0143-1471\(80\)90071-9](https://doi.org/10.1016/0143-1471(80)90071-9)
- 1184 Mitchel, R.H., 1986. Kimberlite and Related Rocks, in: *Kimberlites Mineralogy,*  
1185 *Geochemistry, and Petrology.* Plenum Press, New York, USA, pp. 9–28.
- 1186 Mukiza, E., Zhang, L.L., Liu, X., Zhang, N., 2019. Utilization of red mud in road base and  
1187 subgrade materials: A review. *Resour. Conserv. Recycl.*  
1188 <https://doi.org/10.1016/j.resconrec.2018.10.031>
- 1189 National Academies of Sciences Engineering and Medicine, 2019. *Negative Emissions*  
1190 *Technologies and Reliable Sequestration.* Washington DC.  
1191 <https://doi.org/10.17226/25259>
- 1192 Nordstrom, D.K., Southam, G., 1997. Geomicrobiology of sulfide mineral oxidation. *Rev.*  
1193 *Mineral.* 35, 381–390. <https://doi.org/10.1515/9781501509247>
- 1194 Nowamooz, A., Dupuis, J.C., Beaudoin, G., Molson, J., Lemieux, J.-M., Horswill, M., Fortier,  
1195 R., Larachi, F., Maldague, X., Constantin, M., Duchesne, J., Therrien, R., 2018.  
1196 Atmospheric Carbon Mineralization in an Industrial-Scale Chrysotile Mining Waste Pile.  
1197 *Environ. Sci. Technol.* 52, 8050–8057. <https://doi.org/10.1021/ACS.EST.8B01128>
- 1198 Olabi, A.G., Obaideen, K., Elsaid, K., Wilberforce, T., Sayed, E.T., Maghrabie, H.M.,  
1199 Abdelkareem, M.A., 2022. Assessment of the pre-combustion carbon capture  
1200 contribution into sustainable development goals SDGs using novel indicators. *Renew.*  
1201 *Sustain. Energy Rev.* 153, 111710. <https://doi.org/10.1016/J.RSER.2021.111710>
- 1202 Olszewska, J.P., Meharg, A.A., Heal, K. V, Carey, M., Gunn, I.D.M., Searle, K.R., Winfield, I.J.,  
1203 Spears, B.M., 2016. Assessing the Legacy of Red Mud Pollution in a Shallow Freshwater  
1204 Lake: Arsenic Accumulation and Speciation in Macrophytes.  
1205 <https://doi.org/10.1021/acs.est.6b00942>
- 1206 Oskierski, H.C., Dlugogorski, B.Z., Jacobsen, G., 2013. Sequestration of atmospheric CO<sub>2</sub> in  
1207 chrysotile mine tailings of the Woodsreef Asbestos Mine, Australia: Quantitative  
1208 mineralogy, isotopic fingerprinting and carbonation rates. *Chem. Geol.* 358, 156–169.  
1209 <https://doi.org/10.1016/j.chemgeo.2013.09.001>
- 1210 Oskierski, H.C., Dlugogorski, B.Z., Oliver, T.K., Jacobsen, G., 2016. Chemical and isotopic  
1211 signatures of waters associated with the carbonation of ultramafic mine tailings,  
1212 Woodsreef Asbestos Mine, Australia. *Chem. Geol.* 436, 11–23.  
1213 <https://doi.org/10.1016/j.chemgeo.2016.04.014>
- 1214 Oskierski, H.C., Turvey, C.C., Wilson, S.A., Dlugogorski, B.Z., Altarawneh, M., Mavromatis, V.,  
1215 2021. Mineralisation of atmospheric CO<sub>2</sub> in hydromagnesite in ultramafic mine tailings  
1216 – Insights from Mg isotopes. *Geochim. Cosmochim. Acta* 309, 191–208.  
1217 <https://doi.org/10.1016/J.GCA.2021.06.020>

- 1218 Pade, C., Guimaraes, M., 2007. The CO<sub>2</sub> uptake of concrete in a 100 year perspective. *Cem.*  
1219 *Concr. Res.* 37, 1348–1356. <https://doi.org/10.1016/J.CEMCONRES.2007.06.009>
- 1220 Pan, S.Y., Chang, E.E., Chiang, P.C., 2012. CO<sub>2</sub> capture by accelerated carbonation of alkaline  
1221 wastes: A review on its principles and applications. *Aerosol Air Qual. Res.* 12, 770–791.  
1222 <https://doi.org/10.4209/aaqr.2012.06.0149>
- 1223 Paulo, C., Power, I.M., Stubbs, A.R., Wang, B., Zeyen, N., Wilson, S.A., 2021. Evaluating  
1224 feedstocks for carbon dioxide removal by enhanced rock weathering and CO<sub>2</sub>  
1225 mineralization. *Appl. Geochemistry* 129, 104955.  
1226 <https://doi.org/10.1016/J.APGEOCHEM.2021.104955>
- 1227 Pokrovsky, O.S., Schott, J., 2000. Kinetics and mechanism of forsterite dissolution at 25°C  
1228 and pH from 1 to 12. *Geochim. Cosmochim. Acta* 64, 3313–3325.  
1229 [https://doi.org/10.1016/S0016-7037\(00\)00434-8](https://doi.org/10.1016/S0016-7037(00)00434-8)
- 1230 Poletini, A., Pomi, R., Stramazzo, A., 2016. CO<sub>2</sub> sequestration through aqueous accelerated  
1231 carbonation of BOF slag: A factorial study of parameters effects. *J. Environ. Manage.*  
1232 167, 185–195. <https://doi.org/10.1016/j.jenvman.2015.11.042>
- 1233 Power, G., Gräfe, M., Klauber, C., 2011. Bauxite residue issues: I. Current management,  
1234 disposal and storage practices. *Hydrometallurgy* 108, 33–45.  
1235 <https://doi.org/10.1016/J.HYDROMET.2011.02.006>
- 1236 Power, I., McCutcheon, J., Harrison, A., Wilson, S., Dipple, G., Kelly, S., Southam, C.,  
1237 Southam, G., 2014. Strategizing Carbon-Neutral Mines: A Case for Pilot Projects.  
1238 *Minerals* 4, 399–436. <https://doi.org/10.3390/min4020399>
- 1239 Power, I.M., Dipple, G.M., Southam, G., 2010. Bioleaching of ultramafic tailings by  
1240 *Acidithiobacillus* spp. for CO<sub>2</sub> sequestration. *Environ. Sci. Technol.* 44, 456–462.  
1241 [https://doi.org/10.1021/ES900986N/SUPPL\\_FILE/ES900986N\\_SI\\_001.PDF](https://doi.org/10.1021/ES900986N/SUPPL_FILE/ES900986N_SI_001.PDF)
- 1242 Power, I.M., Harrison, A.L., Dipple, G.M., Wilson, S.A., Kelemen, P.B., Hitch, M., Southam, G.,  
1243 2013. Carbon Mineralization: From Natural Analogues to Engineered Systems. *Rev.*  
1244 *Mineral. Geochemistry* 77, 305–360. <https://doi.org/10.2138/rmg.2013.77.9>
- 1245 Proctor, D.M., Fehling, K.A., Shay, E.C., Wittenborn, J.L., Green, J.J., Avent, C., Bigham, R.D.,  
1246 Connolly, M., Lee, B., Shepker, T.O., Zak, M.A., 2000. Physical and chemical  
1247 characteristics of blast furnace, basic oxygen furnace, and electric arc furnace steel  
1248 industry slags. *Environ. Sci. Technol.* 34, 1576–1582.  
1249 <https://doi.org/10.1021/es9906002>
- 1250 Pronost, J., Beaudoin, G., Constantin, M., Duchesne, J., Hébert, R., 2010. Evaluation of the  
1251 mineral carbonation potential of mining residues produced by Royal Nickel pilot plant,  
1252 Amos.
- 1253 Pronost, J., Beaudoin, G., Lemieux, J.M., Hébert, R., Constantin, M., Marcouiller, S., Klein,  
1254 M., Duchesne, J., Molson, J.W., Larachi, F., Maldague, X., 2012. CO<sub>2</sub>-depleted warm air  
1255 venting from chrysotile milling waste (Thetford Mines, Canada): Evidence for in-situ  
1256 carbon capture from the atmosphere. *Geology* 40, 275–278.  
1257 <https://doi.org/10.1130/G32583.1>
- 1258 Pullin, H., Bray, A.W., Burke, I.T., Muir, D.D., Sapsford, D.J., Mayes, W.M., Renforth, P., 2019.  
1259 Atmospheric Carbon Capture Performance of Legacy Iron and Steel Waste. *Environ. Sci.*  
1260 *Technol.* 53, 9502–9511. <https://doi.org/10.1021/acs.est.9b01265>
- 1261 Ragipani, R., Bhattacharya, S., Suresh, A.K., 2021. A review on steel slag valorisation: Via  
1262 mineral carbonation. *React. Chem. Eng.* 6, 1152–1178.  
1263 <https://doi.org/10.1039/d1re00035g>
- 1264 Renforth, P., 2019. The negative emission potential of alkaline materials. *Nat. Commun.* 10,

- 1265 1401. <https://doi.org/10.1038/s41467-019-09475-5>
- 1266 Renforth, P., 2011. Mineral carbonation in soils : engineering the soil carbon sink. University  
1267 of New Castle.
- 1268 Renforth, P., Manning, D.A.C., Lopez-Capel, E., 2009. Carbonate precipitation in artificial  
1269 soils as a sink for atmospheric carbon dioxide. *Appl. Geochemistry* 24, 1757–1764.  
1270 <https://doi.org/10.1016/j.apgeochem.2009.05.005>
- 1271 Renforth, P., Mayes, W.M., Jarvis, A.P., Burke, I.T., Manning, D.A.C., Gruiz, K., 2012.  
1272 Contaminant mobility and carbon sequestration downstream of the Ajka (Hungary) red  
1273 mud spill: The effects of gypsum dosing. *Sci. Total Environ.* 421–422, 253–259.  
1274 <https://doi.org/10.1016/j.scitotenv.2012.01.046>
- 1275 Renforth, P., Washbourne, C.-L., Taylder, J., Manning, D.A.C., 2011. Silicate Production and  
1276 Availability for Mineral Carbonation. *Environ. Sci. Technol.* 45, 2035–2041.  
1277 <https://doi.org/10.1021/es103241w>
- 1278 Riahi, K., van Vuuren, D.P., Kriegler, E., Edmonds, J., O'Neill, B.C., Fujimori, S., Bauer, N.,  
1279 Calvin, K., Dellink, R., Fricko, O., Lutz, W., Popp, A., Cuaresma, J.C., KC, S., Leimbach, M.,  
1280 Jiang, L., Kram, T., Rao, S., Emmerling, J., Ebi, K., Hasegawa, T., Havlik, P., Humpenöder,  
1281 F., Da Silva, L.A., Smith, S., Stehfest, E., Bosetti, V., Eom, J., Gernaat, D., Masui, T.,  
1282 Rogelj, J., Strefler, J., Drouet, L., Krey, V., Luderer, G., Harmsen, M., Takahashi, K.,  
1283 Baumstark, L., Doelman, J.C., Kainuma, M., Klimont, Z., Marangoni, G., Lotze-Campen,  
1284 H., Obersteiner, M., Tabeau, A., Tavoni, M., 2017. The Shared Socioeconomic Pathways  
1285 and their energy, land use, and greenhouse gas emissions implications: An overview.  
1286 *Glob. Environ. Chang.* 42, 153–168. <https://doi.org/10.1016/j.gloenvcha.2016.05.009>
- 1287 Riley, A.L., MacDonald, J.M., Burke, I.T., Renforth, P., Jarvis, A.P., Hudson-Edwards, K.A.,  
1288 McKie, J., Mayes, W.M., 2020. Legacy iron and steel wastes in the UK: Extent, resource  
1289 potential, and management futures. *J. Geochemical Explor.* 219, 106630.  
1290 <https://doi.org/10.1016/j.gexplo.2020.106630>
- 1291 Riley, A.L., Mayes, W.M., 2015. Long-term evolution of highly alkaline steel slag drainage  
1292 waters. *Environ. Monit. Assess.* 187, 463. <https://doi.org/10.1007/s10661-015-4693-1>
- 1293 Roadcap, G.S., Kelly, W.R., Bethke, C.M., 2005. Geochemistry of Extremely Alkaline (pH > 12)  
1294 Ground Water in Slag-Fill Aquifers. *Ground Water* 43, 806–816.  
1295 <https://doi.org/10.1111/j.1745-6584.2005.00060.x>
- 1296 Roadcap, G.S., Sanford, R.A., Jin, Q., Pardinias, J.R., Bethke, C.M., 2006. Extremely alkaline  
1297 (pH > 12) ground water hosts diverse microbial community. *Ground Water* 44, 511–  
1298 517. <https://doi.org/10.1111/j.1745-6584.2006.00199.x>
- 1299 Santini, T.C., Banning, N.C., 2016. Alkaline tailings as novel soil forming substrates:  
1300 Reframing perspectives on mining and refining wastes. *Hydrometallurgy* 164, 38–47.  
1301 <https://doi.org/10.1016/j.hydromet.2016.04.011>
- 1302 Santos, R.M., Ling, D., Sarvaramini, A., Guo, M., Elsen, J., Larachi, F., Beaudoin, G., Blanpain,  
1303 B., Van Gerven, T., 2012. Stabilization of basic oxygen furnace slag by hot-stage  
1304 carbonation treatment. *Chem. Eng. J.* 203, 239–250.  
1305 <https://doi.org/10.1016/j.cej.2012.06.155>
- 1306 Schott, J., Pokrovsky, O.S., Oelkers, E.H., 2009. The Link Between Mineral  
1307 Dissolution/Precipitation Kinetics and Solution Chemistry. *Rev. Mineral. Geochemistry*  
1308 70, 207–258. <https://doi.org/10.2138/RMG.2009.70.6>
- 1309 Schott, J., Pokrovsky, O.S., Spalla, O., Devreux, F., Gloter, A., Mielczarski, J.A., 2012.  
1310 Formation, growth and transformation of leached layers during silicate minerals  
1311 dissolution: The example of wollastonite. *Geochim. Cosmochim. Acta* 98, 259–281.

- 1312 <https://doi.org/10.1016/J.GCA.2012.09.030>
- 1313 Schuiling, R.D., Krijgsman, P., 2006. Enhanced weathering: An effective and cheap tool to  
1314 sequester CO<sub>2</sub>. *Clim. Change* 74, 349–354. <https://doi.org/10.1007/s10584-005-3485-y>
- 1315 Schuiling, R.D., Wilson, S.A., Power, L.M., 2011. Enhanced silicate weathering is not limited  
1316 by silicic acid saturation. *Proc. Natl. Acad. Sci.* 108, E41–E41.  
1317 <https://doi.org/10.1073/pnas.1019024108>
- 1318 Scott, P.W., Critchley, S.R., Wilkinson, F.C.F., 1986. The chemistry and mineralogy of some  
1319 granulated and pelletized blastfurnace slags. *Mineral. Mag.* 50, 141–148.
- 1320 Si, C., Ma, Y., Lin, C., 2013. Red mud as a carbon sink: Variability, affecting factors and  
1321 environmental significance. *J. Hazard. Mater.* 244–245, 54–59.  
1322 <https://doi.org/10.1016/j.jhazmat.2012.11.024>
- 1323 Song, Q., Guo, M.Z., Wang, L., Ling, T.C., 2021. Use of steel slag as sustainable construction  
1324 materials: A review of accelerated carbonation treatment. *Resour. Conserv. Recycl.*  
1325 173, 105740. <https://doi.org/10.1016/J.RESCONREC.2021.105740>
- 1326 Sorlini, S., Sanzeni, A., Rondi, L., 2012. Reuse of steel slag in bituminous paving mixtures. *J.*  
1327 *Hazard. Mater.* 209–210, 84–91. <https://doi.org/10.1016/j.jhazmat.2011.12.066>
- 1328 Stubbs, A.R., Paulo, C., Power, I.M., Wang, B., Zeyen, N., Wilson, S.A., 2022. Direct  
1329 measurement of CO<sub>2</sub> drawdown in mine wastes and rock powders: Implications for  
1330 enhanced rock weathering. *Int. J. Greenh. Gas Control* 113, 103554.  
1331 <https://doi.org/10.1016/J.IJGGC.2021.103554>
- 1332 Stumm, W., Morgan, J.J., 1996. *Aquatic Chemistry: Chemical Equilibria and Rates in Natural*  
1333 *Waters*, 3rd ed, *Aquatic Chemistry: Chemical Equilibria and Rates in Natural Waters*.  
1334 John Wiley & Sons, Inc.
- 1335 Tayebi-Khorami, M., Edraki, M., Corder, G., Golev, A., 2019. Re-Thinking Mining Waste  
1336 through an Integrative Approach Led by Circular Economy Aspirations. *Minerals* 9, 286.  
1337 <https://doi.org/10.3390/min9050286>
- 1338 Thom, J.G.M., Dipple, G.M., Power, I.M., Harrison, A.L., 2013. Chrysotile dissolution rates:  
1339 Implications for carbon sequestration. *Appl. Geochemistry* 35, 244–254.  
1340 <https://doi.org/10.1016/j.apgeochem.2013.04.016>
- 1341 Tollefson, J., 2018. Sucking carbon dioxide from air is cheaper than scientists thought  
1342 [WWW Document]. URL <https://www.nature.com/articles/d41586-018-05357-w>  
1343 (accessed 2.12.20).
- 1344 Turvey, C.C., Hamilton, J.L., Wilson, S.A., 2018a. Comparison of Rietveld-compatible  
1345 structureless fitting analysis methods for accurate quantification of carbon dioxide  
1346 fixation in ultramafic mine tailings. *Am. Mineral.* 103, 1649–1662.  
1347 <https://doi.org/10.2138/am-2018-6515>
- 1348 Turvey, C.C., Wilson, S.A., Hamilton, J.L., Southam, G., 2017. Field-based accounting of CO<sub>2</sub>  
1349 sequestration in ultramafic mine wastes using portable X-ray diffraction. *Am. Mineral.*  
1350 102, 1302–1310. <https://doi.org/10.2138/am-2017-5953>
- 1351 Turvey, C.C., Wilson, S.A., Hamilton, J.L., Tait, A.W., McCutcheon, J., Beinlich, A., Fallon, S.J.,  
1352 Dipple, G.M., Southam, G., 2018b. Hydrotalcites and hydrated Mg-carbonates as  
1353 carbon sinks in serpentinite mineral wastes from the Woodsreef chrysotile mine, New  
1354 South Wales, Australia: Controls on carbonate mineralogy and efficiency of CO<sub>2</sub> air  
1355 capture in mine tailings. *Int. J. Greenh. Gas Control* 79, 38–60.  
1356 <https://doi.org/10.1016/j.ijggc.2018.09.015>
- 1357 Ul-Hamid, A., 2018. *A Beginners' Guide to Scanning Electron Microscopy*, *A Beginners' Guide*  
1358 *to Scanning Electron Microscopy*. <https://doi.org/10.1007/978-3-319-98482-7>

- 1359 UNSD, 2016. United Nations Statistics Division - Environment Glossary [WWW Document].  
1360 URL <https://unstats.un.org/unsd/environmentgl/gesform.asp?getitem=1178> (accessed  
1361 10.9.20).
- 1362 Urbán, L., Csépli, Z., 2010. Disaster in the Ajka Red Sludge Reservoir on 04 October 2010, in:  
1363 Sixth Meeting of the Conference of He Parties to the Convention on the Transboundary  
1364 Effects of Industrial Accidents. Mol of Hungary.
- 1365 Van Gerven, T., Cornelis, G., Vandoren, E., Vandecasteele, C., Garrabrants, A.C., Sanchez, F.,  
1366 Kosson, D.S., 2006. Effects of progressive carbonation on heavy metal leaching from  
1367 cement-bound waste. *AIChE J.* 52, 826–837. <https://doi.org/10.1002/AIC.10662>
- 1368 Vanderzee, S.S.S., Dipple, G.M., Bradshaw, P.M.D., 2019. Targeting Highly Reactive Labile  
1369 Magnesium in Ultramafic Tailings for Greenhouse-Gas Offsets and Potential Tailings  
1370 Stabilization at the Baptiste Deposit, Central British Columbia (NTS 093K/13, 14).  
1371 *Geosci. BC Summ. Act. 2018 Miner. Min.* 109–118.
- 1372 Wang, X., Ni, W., Li, J., Zhang, S., Hitch, M., Pascual, R., 2019. Carbonation of steel slag and  
1373 gypsum for building materials and associated reaction mechanisms. *Cem. Concr. Res.*  
1374 125, 105893. <https://doi.org/10.1016/J.CEMCONRES.2019.105893>
- 1375 Washbourne, C.-L., Renforth, P., Manning, D.A.C., 2012. Investigating carbonate formation  
1376 in urban soils as a method for capture and storage of atmospheric carbon. *Sci. Total*  
1377 *Environ.* 431, 166–175. <https://doi.org/10.1016/j.scitotenv.2012.05.037>
- 1378 Washbourne, C.L., Lopez-Capel, E., Renforth, P., Ascough, P.L., Manning, D.A.C., 2015. Rapid  
1379 removal of atmospheric CO<sub>2</sub> by urban soils. *Environ. Sci. Technol.* 49, 5434–5440.  
1380 <https://doi.org/10.1021/es505476d>
- 1381 Wilcox, J., Psarras, P.C., Liguori, S., 2017. Assessment of reasonable opportunities for direct  
1382 air capture. *Environ. Res. Lett.* 12. <https://doi.org/10.1088/1748-9326/aa6de5>
- 1383 Wilson, S.A., Dipple, G.M., Power, I.M., Barker, S.L.L., Fallon, S.J., Southam, G., 2011.  
1384 Subarctic Weathering of Mineral Wastes Provides a Sink for Atmospheric CO<sub>2</sub>. *Environ.*  
1385 *Sci. Technol.* 45, 7727–7736. <https://doi.org/10.1021/es202112y>
- 1386 Wilson, S.A., Dipple, G.M., Power, I.M., Thom, J.M., Anderson, R.G., Raudsepp, M., Gabites,  
1387 J.E., Southam, G., 2009a. Carbon dioxide fixation within mine wastes of ultramafic-  
1388 hosted ore deposits: Examples from the Clinton Creek and Cassiar Chrysotile deposits,  
1389 Canada. *Econ. Geol.* 104, 95–112. <https://doi.org/10.2113/gsecongeo.104.1.95>
- 1390 Wilson, S.A., Harrison, A.L., Dipple, G.M., Power, I.M., Barker, S.L.L., Ulrich Mayer, K., Fallon,  
1391 S.J., Raudsepp, M., Southam, G., 2014. Offsetting of CO<sub>2</sub> emissions by air capture in  
1392 mine tailings at the Mount Keith Nickel Mine, Western Australia: Rates, controls and  
1393 prospects for carbon neutral mining. *Int. J. Greenh. Gas Control* 25, 121–140.  
1394 <https://doi.org/10.1016/j.ijggc.2014.04.002>
- 1395 Wilson, S.A., Raudsepp, M., Dipple, G.M., 2009b. Quantifying carbon fixation in trace  
1396 minerals from processed kimberlite: A comparative study of quantitative methods  
1397 using X-ray powder diffraction data with applications to the Diavik Diamond Mine,  
1398 Northwest Territories, Canada. *Appl. Geochemistry* 24, 2312–2331.  
1399 <https://doi.org/10.1016/j.apgeochem.2009.09.018>
- 1400 Wilson, S.A., Raudsepp, M., Dipple, G.M., 2006. Verifying and quantifying carbon fixation in  
1401 minerals from serpentinite-rich mine tailings using the Rietveld method with X-ray  
1402 powder diffraction data. *Am. Mineral.* 91, 1331–1341.  
1403 <https://doi.org/10.2138/am.2006.2058>
- 1404 World Health Organization, 2014. Chrysotile Asbestos [WWW Document]. URL  
1405 [http://www.who.int/ipcs/assessment/public\\_health/chemicals\\_phc](http://www.who.int/ipcs/assessment/public_health/chemicals_phc) (accessed 12.4.20).



- 1406 World Steel Association, 2021. Steel Facts [WWW Document]. URL  
1407 <https://www.worldsteel.org/about-steel/steel-facts.html> (accessed 5.31.21).
- 1408 World Steel Association, 2019. World Steel in Figures 2019.
- 1409 World Steel Association, 2017. Steel Industry co-products [WWW Document]. URL  
1410 [https://www.worldsteel.org/publications/position-papers/co-product-position-](https://www.worldsteel.org/publications/position-papers/co-product-position-paper.html)  
1411 [paper.html](https://www.worldsteel.org/publications/position-papers/co-product-position-paper.html) (accessed 10.14.19).
- 1412 Yang, J., Xiao, B., 2008. Development of unsintered construction materials from red mud  
1413 wastes produced in the sintering alumina process. *Constr. Build. Mater.* 22, 2299–2307.  
1414 <https://doi.org/10.1016/j.conbuildmat.2007.10.005>
- 1415 Yildirim, I.Z., Prezzi, M., 2015. Geotechnical properties of fresh and aged basic oxygen  
1416 furnace steel slag. *J. Mater. Civ. Eng.* 27, 1–11.  
1417 [https://doi.org/10.1061/\(ASCE\)MT.1943-5533.0001310](https://doi.org/10.1061/(ASCE)MT.1943-5533.0001310)
- 1418 You, K., Lee, S.-H., Hwang, S.-H., Kim, H., Ahn, J.-W., 2011. CO<sub>2</sub> Sequestration  
1419 via a Surface-Modified Ground Granulated Blast Furnace Slag Using NaOH Solution.  
1420 *Mater. Trans.* 52, 1972–1976. <https://doi.org/10.2320/matertrans.M2011110>
- 1421 Zevenhoven, R., Kavaliauskaite, I., 2004. Mineral carbonation for long-term CO<sub>2</sub> storage: An  
1422 exergy analysis. *Int. J. Thermodyn.* 7, 23–31.  
1423